Available online at www.sciencedirect.com
SCIENCE DIRECT
International Journal of Multiphase Flow 32 (2006) 527–552
International Journal of Multiphase Flow
www.elsevier.com/locate/ijmulflow

Slug initiation and evolution in two-phase horizontal flow

Priscilla M. Ujang, Christopher J. Lawrence, Colin P. Hale, Geoffrey F. Hewitt *

Department of Chemical Engineering, Imperial College London, Exhibition Rd., London SW7 2AZ, United Kingdom

Received 22 February 2005; received in revised form 27 November 2005

Abstract

A series of two-phase air–water experiments was carried out in order to study the initiation and the subsequent evolution of hydrodynamic slugs in a horizontal pipeline. Experiments were carried out at atmospheric pressure, 4.0 bar(a) and 9.0 bar(a), and the effects of superficial liquid and gas velocities were investigated. The test section used for these experiments is 37 m in length, with an internal diameter of 0.078 m. To study the interfacial development, measurements of interfacial structures were made at 14 axial locations along the test section, with data acquired at a sampling frequency of 500 Hz. A large number of slugs were initiated within the first 3 m of the test section, with the frequency subsequently reducing towards the fully developed value before the end of the pipe. This reduction in frequency was strongly influenced by the magnitude of the gas and liquid velocities. The frequency of slugging was not strongly affected when the system pressure was changed from 1 atmosphere, to 4.0 and 9.0 bar(a), closely similar values being obtained at the 10 downstream locations. However, higher pressure delayed the onset of slug initiation, with "slug precursors" being formed further downstream as the pressure was increased. The statistical distributions of slug lengths and of the time intervals between slug arrivals were examined in detail and compared to several standard distributions. This showed that slug initiation may be reasonably approximated as an uncorrelated Poisson process with an exponential distribution of arrival times. However, once slugs have developed, there is strong correlation and the arrival time intervals, as well as the lengths, are best represented by the log-normal distribution.

Keywords: Slug initiation; Gas–liquid horizontal flow

1. Introduction

Slug flows can be classified into two main groups: hydrodynamic and terrain slugging. Hydrodynamic slugging is the normal slugging pattern encountered in straight flow lines. Terrain slugging results from liquid accumulation in local dips of flow lines with variable topography. In many experimental studies of hydrodynamic slugging, the entrance to the pipeline is arranged to give a stratified flow, in which the gas flows above the liquid in parallel streams, and slugs originate from waves at the gas–liquid interface that grow to fill the pipe cross-section. An accepted mechanism for this wave growth is the Kelvin–Helmholtz instability; where

* Corresponding author. Tel.: +44 (0) 2075945562; fax: +44 (0) 2075945564.
E-mail address: g.hewitt@imperial.ac.uk (G.F. Hewitt).

0301-9322/$ - see front matter © 2006 Elsevier Ltd. All rights reserved.
doi:10.1016/j.ijmultiphaseflow.2005.11.005

the interface is elevated, the local gas velocity increases so that the gas pressure reduces, and this suction tends to further elevate the interface, increasing the wave amplitude. The wave growth is opposed by gravity, and this gives rise to a criterion for instability, where the gas velocity is sufficient to overcome gravity. Surface tension also opposes wave growth, but acts on a length-scale that is too small to directly influence the formation of slugs.

Once formed, slugs initially grow in length, with their fronts traveling faster than their tails. It is possible for a slug to continue growing all the way along the pipe; this typically occurs for the first slug initiated in a stratified system, since the thickness of the liquid layer in front of it is high enough to sustain growth at the front. As the cycle of wave growth and slug initiation repeats, subsequent slugs can only pick-up the liquid shed by previous slugs, and may approach a constant length in which the front and tail velocities are equal. The tails of short slugs tend to move faster and this may lead to the slugs becoming shorter and ultimately degenerating into large amplitude waves. These residual waves can be overtaken and consumed by subsequent slugs (increasing their growth), so that the number of slugs tends to reduce in the downstream direction. This has been described by Hale et al. (2001) in terms of competition between slugs and survival of the "fittest" (i.e. largest) slugs. The formation, growth, and decay of slugs is thus highly complex, particularly in the entrance region.

Many authors have addressed the mechanisms of slug formation and established approximate criteria for the transition from stratified to slug flow. Other authors have established correlations of experimental data, or heuristic models for the frequency of slugs in "fully developed" flow. The frequency is related to the mean of the distribution of the time intervals between slugs, and other authors have reported details of this distribution, as well as the associated distribution of slug lengths, again for fully developed flow. However, very little is known of the characteristics of slugs in the region where they are initiated and developed. The purpose of the present paper is to report an experimental examination of the statistics of slugs in the initiation region, and the development of these statistics along a pipeline towards fully developed flow. Knowledge of the evolution of slug statistics along a pipeline is important for the assessment of slug initiation and evolution models, such as the slug capturing models (e.g. Issa and Kempf, 2003) and slug tracking models (e.g. Nydal and Banerjee, 1996).

The onset of the wavy flow regime in gas–liquid pipeline flows is often modeled using a form of the long-wave Kelvin–Helmholtz analysis. The classical Kelvin–Helmholtz instability occurs in stratified flow of two incompressible inviscid fluids, of different densities and velocities, in horizontal layers of infinite depth. The inviscid Kelvin–Helmholtz (IKH) analysis of stratified pipeline flow was first reported by Taitel and Dukler (1976). However a viscous Kelvin–Helmholtz (VKH) analysis, including the effects of wall and interfacial shear stress, generally gives better predictions for the onset of slug flow (Lin and Hanratty, 1986; Hall, 1992; Crowley et al., 1992; Barnea and Taitel, 1994a,b; Funada and Joseph, 2001). But if the viscosity difference between the two fluids is very large, this analysis has been found to fail (McCready, 1998). Several other wave generation theories have been proposed, such as those of Jeffreys (1924, 1925), Benjamin (1959), Lighthill (1962) and Belcher and Hunt (1993). The basis of these theories is the transfer of energy from the gas to the liquid across the perturbed surface, which is related to the pressure and shear stress distributions on the surface of a wave. These theories may predict wave growth at lower gas velocities than the Kelvin–Helmholtz approach.

Visual observations of wave growth and slug formation show that the slugs are formed from long waves, when they become large enough to bridge the pipe-cross-section (Taitel and Dukler, 1977; Kordyban, 1985; Lin and Hanratty, 1987; Andritsos and Hanratty, 1987; Woods and Hanratty, 1999). It may be significant that the surface of the long waves tends to be roughened by additional small amplitude short waves. Several models have been proposed for the frequency of slug initiation, one of the first being the model of Taitel and Dukler (1977). This model emphasizes the importance of the rebuilding of the liquid layer left behind by a newly formed slug as it accelerates away after the bridging event. Subsequent models (Woods and Hanratty, 1999; Hale, 2000) have adopted a similar concept of the development of the liquid level to determine the bridging frequency. The Taitel and Dukler (1977) and Hale (2000) models are based on the one-dimensional two-fluid model equations, while the model of Woods and Hanratty (1999) follows a stochastic approach.

Taitel and Dukler (1977) explained the initiation process as follows; long wavelength disturbances on a stratified layer develop into growing waves until eventually one of the waves grows to momentarily block

the pipe. This restricts the flow of gas and so pressure builds up behind the blockage, causing it to be accelerated to the gas velocity, forming a short slug, referred to as a "pseudo-slug" or a "slug precursor". The liquid level behind the slug precursor is somewhat depleted and some time is needed to replenish it; enabling the cycle to repeat. Meanwhile, the slug precursor advances downstream. If the rate at which liquid is picked up at the slug front is greater than the rate at which liquid is shed at the tail, the slug precursor grows in length to form a "fully developed" slug. However, if the rate of shedding at the tail is greater than the rate of pick-up at the front, the slug precursor is ephemeral and collapses back into a large wave. Based on this description, Taitel and Dukler (1977) proposed a model to calculate the initiation frequency in terms of the time between successive pipe-bridging events. According to Taitel and Dukler, this time is composed of two parts; once the liquid height has built to its equilibrium level, there is the time, t_1, for a wave to bridge the pipe and the liquid to drop to its lowest level. After this has occurred, there is then the additional time, t_2, for the layer to rebuild to its equilibrium level. From visual observations of the two processes, Taitel and Dukler concluded that t_1 is very short compared to the overall cycle time. Almost immediately after the level rebuilds to its equilibrium value, a wave moves across the liquid surface and bridges the pipe. Since the frequency of the waves is an order of magnitude higher than the slug frequency, bridging takes place almost immediately after the equilibrium level is re-established. Consequently, they consider the liquid rebuild time to be characteristic of the overall cycle time and conclude that the problem of predicting the slug frequency reduces to that of determining the time for the liquid to rebuild from its lowest level. The equilibrium liquid height, $h_{Lf,e}$, was calculated by an iterative solution of the steady-state momentum balances. Since large waves were never seen when the liquid was at its minimum level, this lowest level, $h_{Lf,min}$, was assumed to be given by the neutral stability condition of Taitel and Dukler (1976). They chose this level instead of the minimum level behind the preceding slug because their visual observations suggested that, under the conditions of slug formation, the minimum liquid level was different from that predicted by Dukler and Hubbard (1975) steady-state slug flow model.

Woods and Hanratty (1999) investigated the effect of the liquid Froude number on slug initiation for air–water flow in a horizontal pipe of length 20 m and internal diameter 0.076 m. The transient characteristics of the flow were determined by simultaneous measurements of the liquid holdup at multiple locations. Their study revealed that the mechanisms of slug formation, and thus the slug frequency, depend on the liquid Froude number of the wavy stratified flow, the gas velocity and the bridging location, but their results did not support the proposals of Taitel and Dukler (1977). Woods and Hanratty (1999) presented their results for slug initiation in terms of three distinct zones on a map of U_{SG} and U_{SL}. In the first zone, the Froude number was less than unity and slugs were initiated at a distance more than 40 times the pipe diameter. In the second zone, the Froude number was greater than unity but slugs were still initiated at similar locations. In the final zone, the Froude number was greater than unity and slugs were formed at a distance less than 40 times the diameter. Their stochastic model was developed for slug initiation in the two cases where the liquid Froude number was greater than unity.

Davies (1992) and Hale (2000) carried out flow-visualization studies of the initiation process using a horizontal transparent Perspex pipe of length 10 m and internal diameter 0.074 m. Stratified flow of liquid and gas at the inlet was achieved using a horizontal dividing plate. In the study of Davies (1992), a high speed video camera operating at 1000 frames/s was placed near the pipe entrance. The refractive index mismatch between the pipe material and the water was reduced by using a length of fluorinated ethylene propylene (FEP) tubing of refractive index 1.34 at the visualization location. The FEP pipe was encased within an external box filled with water. A series of photographs from one of these experiments is shown in Fig. 1. The dashed vertical lines in each image are 0.02 m apart. From these and similar pictures, it was observed that the distance traveled by the growing wave prior to bridging is very short (typically one or two diameters). These observations also showed that it is possible for small amplitude waves to ride on top of the rebuilding liquid layer and continue to develop as they advance over the sloping surface.

Davies (1992) proposed the following mechanism for slug initiation. He suggested that there is a position, x_I, downstream of the pipe inlet at which unstable waves first appear. These waves advance downstream from this position and continue to grow until one is of sufficient size to bridge the pipe at position, x_B. The liquid blockage created by this bridging event is then accelerated by the gas, forming a short slug precursor, which advances rapidly over the liquid profile left by the preceding slug. The slug precursor will grow as long as there is sufficient liquid available for the pickup rate at its front to be larger than the shedding rate at its tail. Behind

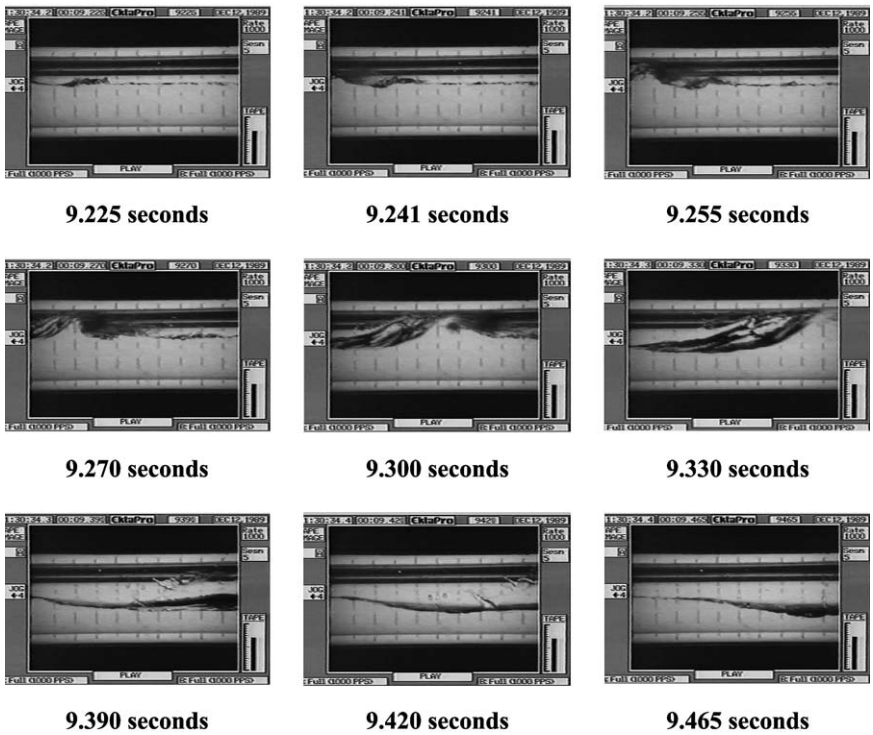

Fig. 1. Time series of photographs of a wave bridging event ($U_{SG} = 1.84$ m/s, $U_{SL} = 0.30$ m/s) (from Davies, 1992).

the slug precursor, the liquid layer has a gradient from a height determined by the amount of liquid shed at its tail to the equilibrium level at x_I. Meanwhile, the liquid inflow rebuilds the level downstream of the position x_I. Unstable waves are continually initiated at position x_I, and travel over the rebuilding surface, growing until they reach the neutral stability point x_S, at which the liquid height is below the level necessary for waves to grow. Once the waves pass the neutral stability point x_S, their amplitude decays and they eventually disappear. However, as the liquid level rebuilds, the point x_S moves downstream, and there is greater opportunity for pipe bridging before the wave reaches x_S. For a fixed set of flow conditions this means that the axial position of successive wave bridging events may vary.

Using two high speed cameras at 1.75 m and 5.60 m from the inlet and observing a length of 1.5 pipe diameters with each, Hale (2000) observed a reduction in slug frequency along the pipe. Some of the slug precursors collapse so that the liquid level remains almost constant for considerable periods of time in the downstream region.

The measurement of representative slug statistics requires careful experimentation and several precautions must be taken to eliminate artifacts of the experiment. As well as the detailed events of slug initiation in the pipe inlet region, the slug frequency observed in experiments may also be influenced by the transit time of slugs through the pipe, especially in short test sections. Besides the reduction in the liquid level after a slug precursor is formed, each slug influences the initiation process in a more subtle way – by increasing the pressure in the inlet region. In the WASP facility, where the experiments described in the present paper were carried out, the inlet gas and liquid mass flow rates are independent of the test section pressure, but this is not universally the case. If the flow rate is not held constant, then significant oscillations can occur as the pressure fluctuates, so that slug initiation becomes a property of the experimental facility, rather than a property of the flow itself.

Even when the flow rates are fixed, as in the WASP facility, the exit of each slug from the pipeline is accompanied by an upstream-propagating pressure wave that can influence the conditions near the inlet. If the pipe is long enough, it may also be assumed that the slug residence time in the pipe is significantly greater than the

time it takes for the stratified layer to rebuild following a bridging event. For a flow condition in which the gas velocity is only slightly above the critical value for slug flow, unstable waves will be formed. Once one of these waves grows to form a "slug precursor", the pressure in the upstream gas pocket will increase. This will result in a decrease in the gas velocity and hence a rise in the liquid level due to reduced interfacial shear. The expected local flow pattern upstream of the slug may therefore be stratified flow because the gas velocity will be below the critical value necessary for the transition to intermittent flow. As a result, no new slug will form when the liquid height rebuilds. However, once a slug in the downstream region leaves the pipe, the gas pressure upstream will be reduced, leading to a condition where the gas velocity is greater and the liquid height higher than before. As a result, waves will grow rapidly to form a new slug. This new slug will encounter the slightly higher liquid level as it moves downstream and so will tend to grow. The pressure upstream will once more increase due to the presence of the new slug and the cycle will repeat. This effect will be present, though muted, even when the flow is well into the slug flow regime. The only way to suppress it is to have a pipeline long enough to contain many slugs at a given time, so that the effect of each one is reduced. In some experimental facilities, the transit time of the slug will be similar to or even shorter than the interface rebuilding time. In such cases, there is at most one slug in the pipeline at any given time, and an artificially high slug frequency may be observed.

The initiation of slugs in gas–liquid slug flow has been the subject of much study and some controversy. Major problems can arise in distinguishing between large waves and slugs with significant gas content, which is not feasible on the basis of instantaneous measurements of local liquid holdup alone. This paper describes a study of slug initiation and development in horizontal air–water slug flows in which the inlet conditions were controlled to give parallel, stratified flow at the pipe inlet with constant mass flow rates, in which a large number of holdup sensors were placed along the pipe. Measurements of the transient characteristics were made very near the inlet, so that the position of slug initiation for given gas and liquid flow rates could be identified with reasonable precision. A crucial feature of the experiments was the use of these sensors to identify the *velocity* of structures (waves or slugs). This was subsequently used as an aid in discriminating between slugs and waves; thus, structures having velocities greater than the mixture velocity were identified as slugs, whereas structures traveling at lower velocities were identified as waves. Compared to conventional means of using a liquid holdup threshold to identify slugs, this approach provides a significant improvement in the identification and counting of the slugs. In what follows, the experimental equipment is described in Section 2. The technique for distinguishing between waves and slugs is described in detail in Section 3. Results for interfacial development are presented in Section 4 and for the evolution of slug frequency in Section 5. Probability density functions for slug arrival times and slug lengths are presented in Section 6. The fits of several standard statistical distributions to these data have been examined and the key results are presented. Finally, the conclusions of this work are presented in Section 7.

2. Description of the experiments

The experiments were carried out in the test section of the Imperial College WASP High Pressure Multiphase Flow Facility, using air and water. This is a stainless steel pipe of internal diameter 0.078 m, and length 37 m, which was carefully aligned to be horizontal for the present experiments. The WASP facility operates on a blowdown principle in which high-pressure air is introduced to the system in a controlled manner to produce the required flow rates. In any one experiment, the maximum amount of air available is 60 m^3 at a pressure of 30 bar(g). The air is also used to pressurize the water storage tank, to assist a centrifugal pump in maintaining a constant water flow rate. Full details of the experiments are given by Ujang (2003).

The air supply is choked to obtain critical flow in the air inlet line so that a known constant (mass) flow rate of gas is introduced. In order to maintain a stable air flow rate during the course of an experiment, the air supply pressure is maintained above 20 bar(a) and the ratio between the upstream and downstream pressures at the choke is maintained above 1.9, which is the critical value for air at ambient temperature. The water flow rate is fixed through a control valve and measured with a magnetic flow meter before its introduction into the test section. The phases are introduced into the test section through an inlet piece shown in Fig. 2, which is a short length of modified testline that connects smoothly with the main test section. There are three individual inlets; one each for air, water and oil (the oil was not used in these experiments). In order to enhance the initial

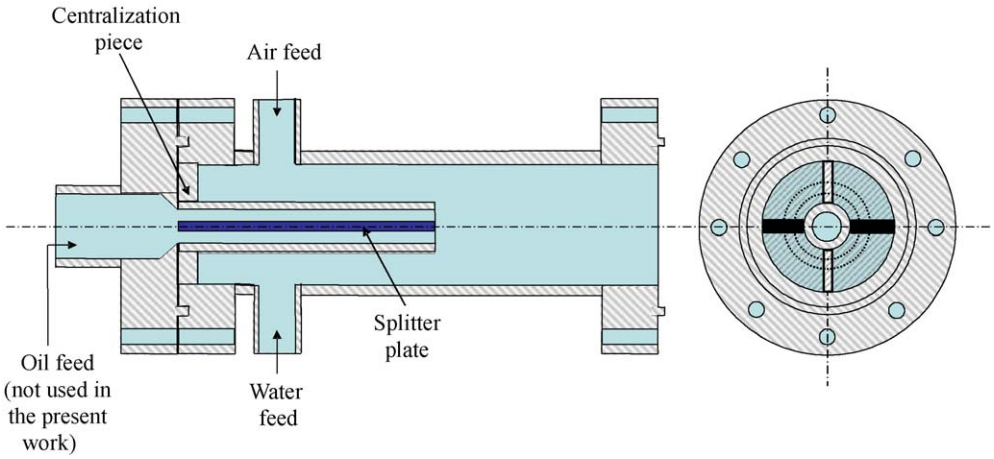

Fig. 2. The inlet to the test section (not to scale).

stratification of the feed, the inlets are arranged so that each phase is introduced at a point governed by its relative density: air is fed perpendicularly into the top of the section and water perpendicularly into the bottom. The phases are aligned into stratified flow by a splitter plate arranged across the horizontal diameter of the pipe.

From the main testline, the fluid discharges into a slug catcher where phase separation occurs at pressure. The slug catcher is a pressure vessel equipped with baffles welded to annular plates to absorb the momentum of the liquid, while reducing any feedback oscillation in the back pressure and designed to promote slug break-up. The air is discharged from the slug catcher through a control valve and a silencer. The liquid drains from the bottom of the slug catcher through a flow control valve and discharges into a dump tank. The facility is operated via a computer control system; further details are given by Hale (2000).

The facility is equipped with instrumentation for the monitoring of temperature, pressure, pressure gradient and liquid level. Four thermocouples were used to measure the temperature in the air and water feed lines, and at approximately 5 m and 30 m downstream from the inlet of the test section. Four absolute pressure transducers were located just downstream of the air flow measurement and at 2.5 m, 21 m and 36 m from the inlet, with ranges of 0–75 bar(a), 0–50 bar(g), 0–20 bar(g) and 0–20 bar(g), respectively. The pressure gradient was measured with a differential pressure transducer, over a range of 2.2 m, centred at 33 m from the inlet. A visualization section, fitted at 35 m, near the downstream end of the test section allowed video recording of the flow. The development of slugs was tracked using conductivity probes which measured the liquid height at 15 axial locations in the flow.

Four designs of conductivity probes were used in the present study (Fig. 3). The original design by Manolis (1995) (Fig. 3a) has two parallel stainless steel wires, positioned 0.002 m apart, across the vertical diameter of the pipe cross-section. These wires are strung through a brass plug and insulated by PTFE, silicone rubber and ceramic insulators. Each plug is then covered with a copper cover and mounted onto one of several steel reinforcing rings placed at intervals along the test section. Six of these probes were used within the first 7 m of the test section, and another two at 26 m and 27 m from the inlet. The second design is by Srichai (1994) (Fig. 3b) and consists of multiple sets of twin-wires stretched across vertical chords of the pipe. In this design, five pairs of wires are mounted on an annular acrylic holder which is secured between two ANSI 600 tongue and groove flanges in the test section. Four probes are spaced ± 0.0128 m and ± 0.0256 m from the central diametrical probe. The third design, by Shaha (1999), has three pairs of stainless steel wires placed in one half of the cross-section of the pipe, and the fourth design (Hale, 2000) has just a central twin-wire probe. The third and fourth designs have the same mounting as the second (Srichai, 1994). In all four designs, the separation of the wires in each pair is 0.002 m. All of the probes were calibrated off-line prior to the experiments, but only the central diametrical probe of the multiple-probe assemblies was used for the measurements reported here.

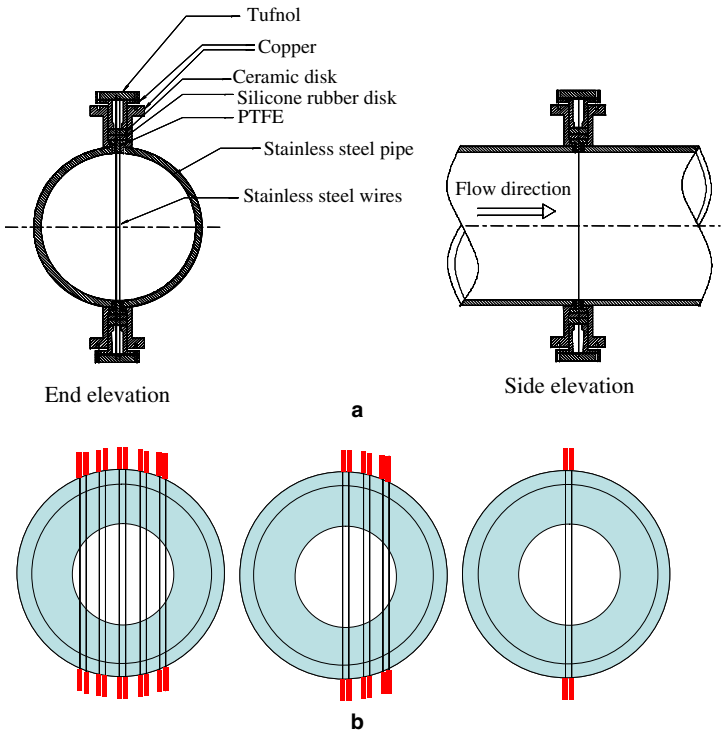

Fig. 3. WASP conductivity probe design: (a) type 1 (Manolis, 1995; Ujang, 2003) (the reinforcement ring is not shown for clarity); (b) types 2, 3 and 4 (Srichai, 1994; Shaha, 1999; Hale, 2000).

3. Discrimination between slugs and waves

The most direct means of identifying slugs from a time series of liquid height measurements is to choose objects characterised by a sharp rise in liquid height at the front and a sharp drop in height at the back, whose liquid holdup is close to unity. In fully developed slug flow, the differences between waves and slugs are clear; slug signals are more rectangular than those due to waves. However, in the initiation region, where the new slugs are still very short, a more sophisticated method of identification is required. A characteristic of a new slug is that the liquid layer ahead of it is relatively deep, while the liquid height drops sharply behind its tail. In contrast, large waves normally show a more gradual decrease of liquid height in their tail profile. Both slugs and waves, however, have very short lengths, and discrimination between slugs and waves based on the liquid height alone is quite problematic.

In the present work, valuable additional information has been obtained by estimating the translational velocity of each object. The propagation velocity of slugs is at least equal to the mixture velocity, whereas waves tend to move more slowly. The arrival times of each wave or slug (i.e. all major peaks in the time series of liquid height) at each probe location were recorded and matched with the corresponding times for the probe immediately downstream. These signals were then cross-correlated in order to obtain the average translational velocity. For a discrete time series, the cross-correlation function is given by

$$R_{xy}(\tau) = \frac{1}{N-j}\sum_{i=1}^{N-j} x_i y_{i+j} \tag{1}$$

where $\tau = j\Delta t$ is the time delay, Δt is the sampling interval of the data and N is the number of data points in the segment to be correlated. Each segment of data was first normalized by subtracting the segment mean and dividing by the segment standard deviation. In the present work, separate time segments were used for the

upstream $\{x_i\}$ and downstream $\{y_i\}$ data segments to ensure that only one slug or wave feature occurred within each window. Eq. (1) is then modified to the following form:

$$R_{xy}(\tau) = \frac{1}{N-j}\sum_{i=1}^{N-j} x_i y_{i+j+k} \tag{2}$$

where the offset k is the number of data points separating the starting points of the upstream and downstream data segments, and N is the size of the smaller segment. Examples of the segments used are shown in Fig. 4a, where the upstream and downstream probes are a distance $L = 6.05$ m apart. The corresponding cross-corre-

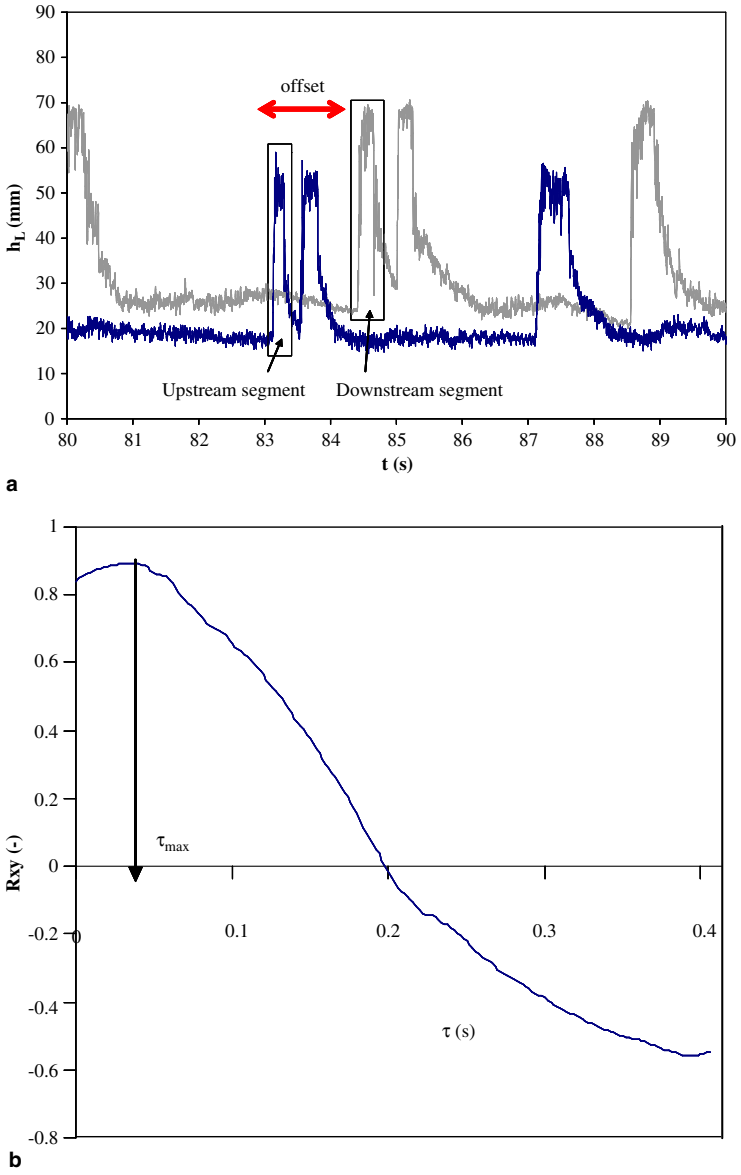

Fig. 4. (a) Example of the time segments used in cross-correlating signals between upstream and downstream probes. (b) Cross-correlation function for the data segments shown in (a).

lation function for these data is shown in Fig. 4b, and the time delay τ_{max} that maximises the correlation, is identified. The object velocity is then determined using

$$u_{corr} = \frac{L}{k\Delta t + \tau_{max}} \tag{3}$$

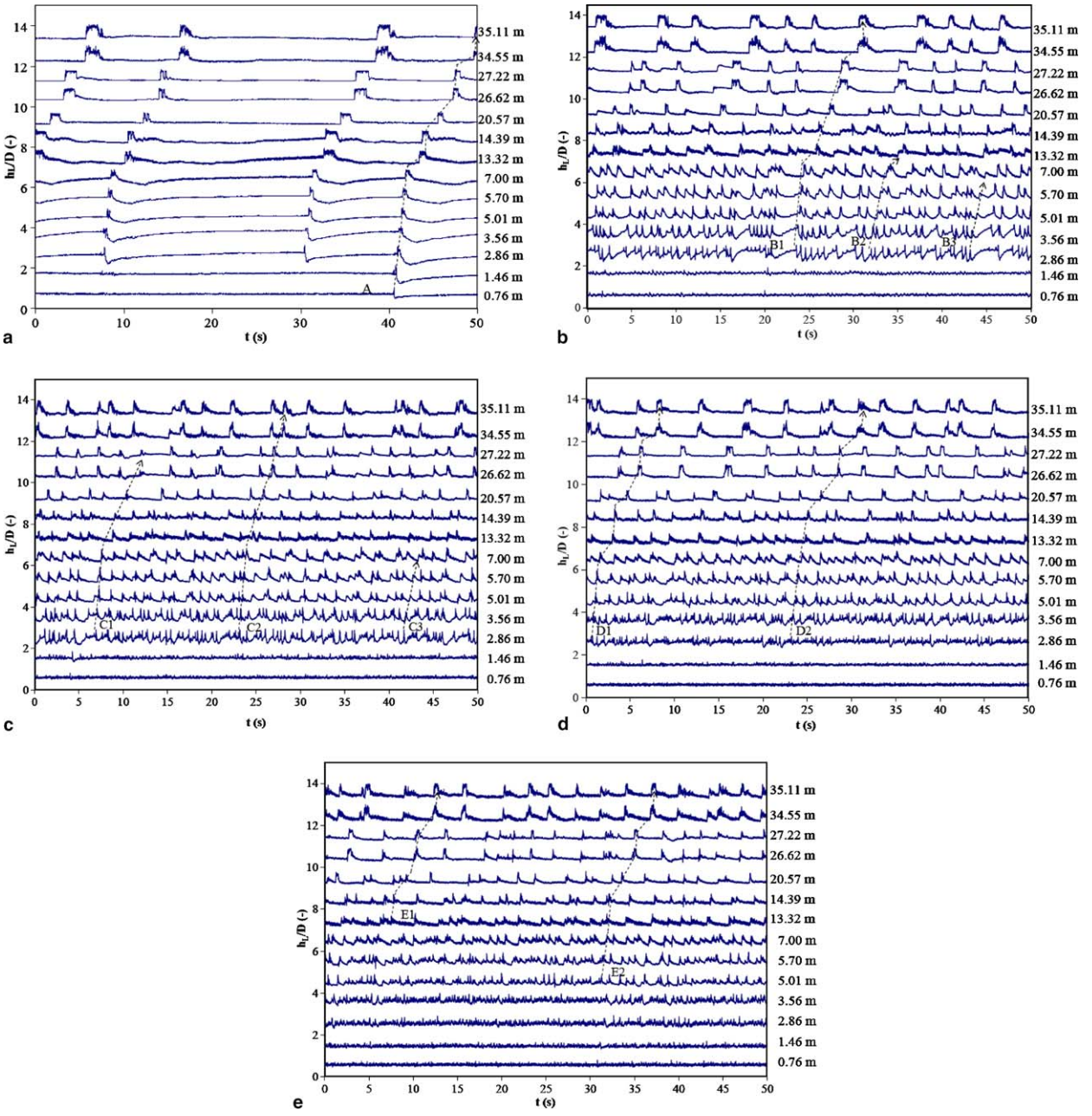

Fig. 5. Time series of dimensionless liquid height illustrating the interfacial development along the test section. The trace for each probe after the first is offset by unity from its upstream neighbour. (a) $U_{SL} = 0.22$ m/s, $U_{SG} = 2.27$ m/s, inlet pressure = 1.04 bar(a); (b) $U_{SL} = 0.61$ m/s, $U_{SG} = 2.55$ m/s, inlet pressure = 1.11 bar(a); (c) $U_{SL} = 0.61$ m/s, $U_{SG} = 4.64$ m/s, inlet pressure = 1.15 bar(a); (d) $U_{SL} = 0.62$ m/s, $U_{SG} = 2.43$ m/s, inlet pressure = 4.70 bar(a); (e) $U_{SL} = 0.61$ m/s, $U_{SG} = 2.55$ m/s, inlet pressure = 8.96 bar(a).

The actual front and tail velocities of a slug, when required, were determined by subjectively identifying the arrival times of its front and tail at two adjacent probes, and dividing the probe separation distance by the respective time differences.

4. Development of the interfacial profile

Measurements from the conductivity probes showing the growth of waves into slugs, and the subsequent evolution of these slugs are shown for several flow conditions in Fig. 5. Fig. 5a shows a base case with superficial liquid velocity $U_{SL} = 0.22$ m/s, superficial gas velocity $U_{SG} = 2.27$ m/s, and test section inlet pressure = 1.04 bar(a). Fig. 5b–e shows the independent effects of increasing superficial liquid velocity (b), superficial gas velocity (c) and inlet pressure (d) and (e) on the development of the interfacial profile along the test section. The results corresponding to the lowest velocity conditions investigated in these experiments are shown in Fig. 5a. A large wave (A) is visible in the signal from the first probe, and this eventually forms a slug that propagates to the exit of the pipe. An interesting feature of this trace is that this slug is initiated very near the inlet (before 0.76 m). The presence of other slugs in the time series for the third probe shows that most of the initiations occur between 1.46 m and 2.86 m. When the superficial liquid velocity is increased to 0.61 m/s, as shown in Fig. 5b, several large waves (e.g. B1, B2, B3) are observed trailing behind slug precursors and propagating on the rebuilding film. Wave B1 eventually becomes a slug, while waves B2 and B3 disappear after 13 m from the inlet. An increase in gas velocity to 4.64 m/s (Fig. 5c), roughens the gas–liquid interface, with the presence of large amplitude waves (C1, C2, C3). However, only a few of the peaks correspond to slugs and an increase in the gas velocity generally reduces the slug frequency. Increasing the pressure to 4.70 bar (Fig. 5d) and 8.96 bar (Fig. 5e) reduces the number of slugs near the inlet, and delays slug initiation to positions further downstream. However there is very little discernible effect of the pressure on the interfacial behaviour in the latter part of the test section.

The experimental time series shown in Fig. 5a–c are consistent with the results of a similar study (Woods, 1998; Woods and Hanratty, 1999), using a shorter pipe of very similar diameter at atmospheric pressure. The authors reported that for low liquid and moderate gas superficial velocities ($U_{SL} = 0.1$–0.3 m/s, $U_{SG} = 1.0$–7.0 m/s), slugs were initiated from interfacial instabilities far downstream of the inlet (cf. Fig. 5a). At higher liquid velocities ($U_{SL} = 0.35$–1.0 m/s) and the same gas velocities (cf. Fig. 5b and c), slugs were observed to initiate from disturbances generated at the inlet. For slug flows at high liquid and very low gas velocities ($U_{SL} = 0.4$–1.0 m/s, $U_{SG} = 1.0$–2.5 m/s), the flows were well developed from a distance 200 times the pipe diameter onwards (cf. Fig. 5b).

Fig. 6 shows the evolution of the front and tail velocities, and slug length, for individual slugs followed along the test section. Fig. 6a, shows the properties of a slug from Fig. 5a, for superficial velocities $U_{SL} = 0.22$ m/s and $U_{SG} = 2.27$ m/s. The front velocity is initially much higher than the tail velocity, facilitated by the very thick layer of liquid ahead of the slug, which leads to a rapid growth of the slug. After about

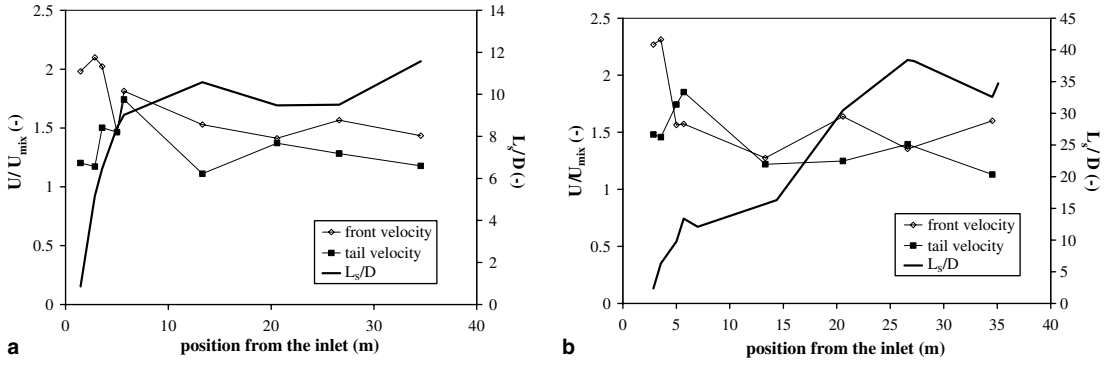

Fig. 6. Evolution of the front and tail velocities and lengths of a representative slug: (a) $U_{SL} = 0.22$ m/s, $U_{SG} = 2.27$ m/s, inlet pressure = 1.04 bar(a); (b) $U_{SL} = 0.61$ m/s; $U_{SG} = 2.55$ m/s, inlet pressure = 1.11 bar(a).

10 m, the slug attains a roughly constant length with $L_s/D \sim 10$. Fig. 6b shows the properties of a slug from Fig. 5b, for $U_{SL} = 0.61$ m/s and $U_{SG} = 2.55$ m/s. This has a similar steady growth phase to about $L_s/D \sim 38$ by about 25 m. Fig. 6 demonstrates the actual evolution of individual slugs, which is unseen in common statistical representations of slug flow properties.

5. Evolution of slug frequency along the pipeline

The effect of the superficial gas and liquid velocities on the evolution of slug frequency along the pipeline is illustrated in Figs. 7 and 8. Each panel of Fig. 7 shows data for a single superficial liquid velocity and several gas velocities. In each case, there are no (or a very small number of slugs for the lowest superficial liquid velocity case) slugs at the first measuring point, but a large number of slugs form between 2 and 3 m,

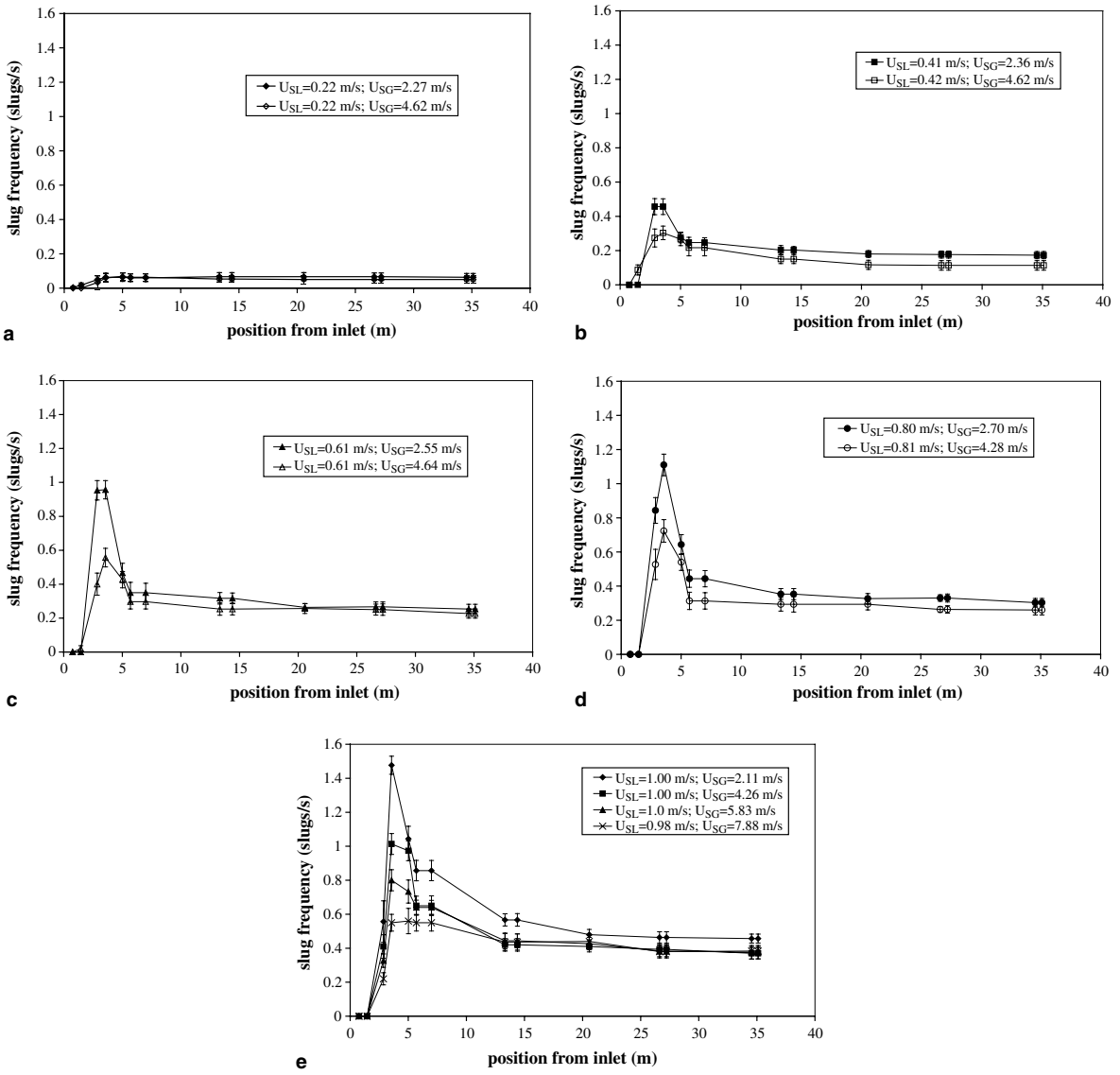

Fig. 7. The effect of superficial gas velocity on the evolution of slug frequency along the pipeline: (a) $U_{SL} = 0.22$ m/s; (b) $U_{SL} = 0.41$ m/s; (c) $U_{SL} = 0.61$ m/s; (d) $U_{SL} = 0.80$ m/s; (e) $U_{SL} = 1.0$ m/s; All data shown are for inlet pressures near atmospheric.

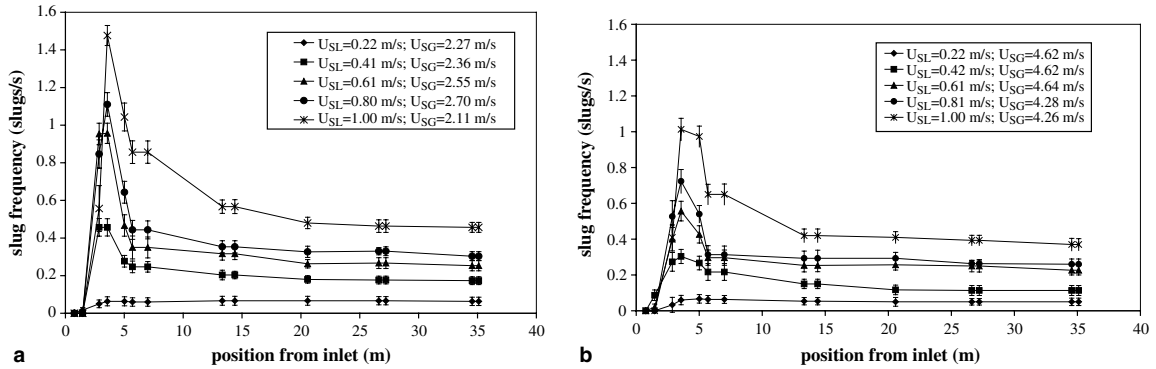

Fig. 8. The effect of superficial liquid velocity on the evolution of slug frequency along the pipeline: (a) $U_{SG} \sim 2$ m/s, (b) $U_{SG} \sim 4$ m/s. All data shown are for inlet pressures near atmospheric.

and the frequency rises to a sharp peak between 3 and 5 m along the pipe. There is then a rapid reduction in slug frequency, followed by a gradual decline as the excess slugs decay and the fully developed slug frequency is recovered. At the lowest superficial liquid velocity, the peak in frequency is absent, and it seems that almost all of the slugs generated near the inlet survive to the end of the pipeline, so the fully developed slug frequency in this case is dictated by the initiation process. As the superficial liquid velocity increases, there is a consistent increase in both the peak slug frequency and the final fully developed value. When the superficial gas velocity is increased from about 2 to 4 m/s, the slug frequency reduces at all points along the pipeline. At

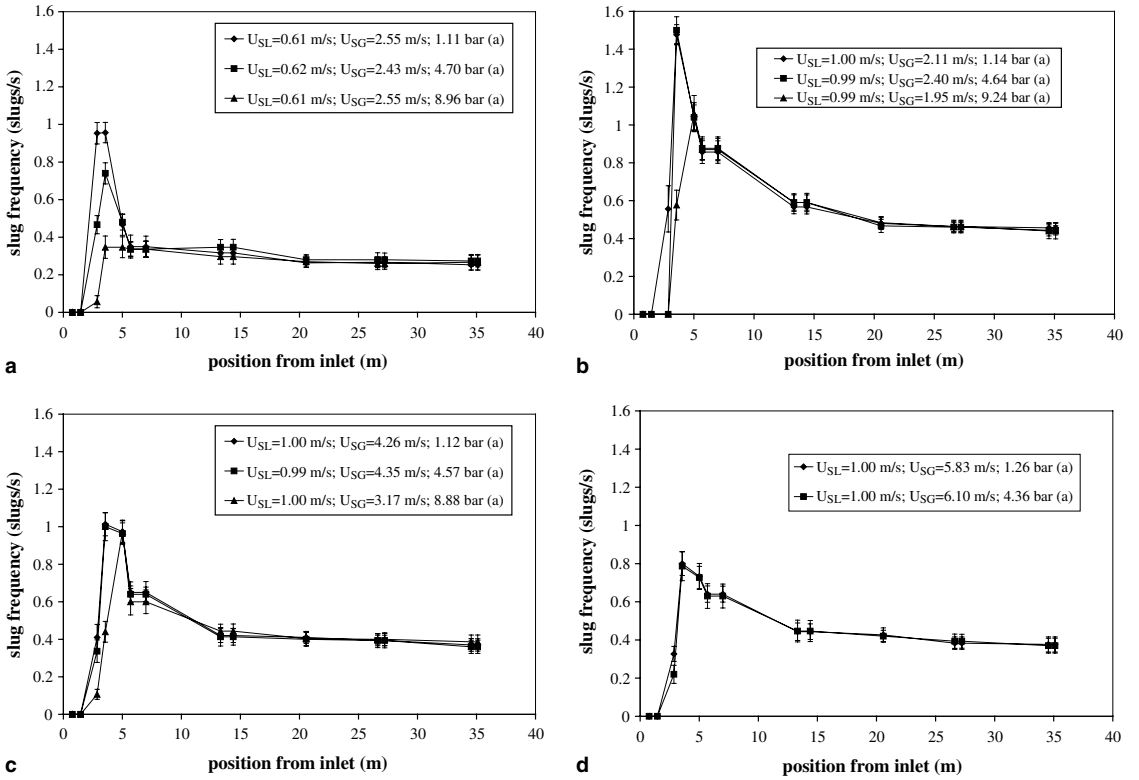

Fig. 9. The effect of pressure on the evolution of slug frequency along the pipeline: (a) $U_{SL} = 0.61$ m/s, $U_{SG} \sim 2.5$ m/s; (b)–(d) $U_{SL} = 1.0$ m/s; (b) $U_{SG} \sim 2$ m/s; (c) $U_{SG} \sim 4$ m/s; (d) $U_{SG} \sim 6$ m/s.

the highest superficial liquid velocity (1 m/s), further increases in the superficial gas velocity to about 6 and 8 m/s lead to a reduction of the peak slug frequency, while the fully developed value is unaffected. It is clear that the superficial gas velocity has a much stronger effect on the slug initiation frequency than on the fully developed slug frequency. Each panel in Fig. 8 shows data for a narrow range of superficial gas velocities and several values of the superficial liquid velocity. This clearly shows that the fully developed slug frequency increases in proportion to the superficial liquid velocity, while the effect on the peak frequency appears to be stronger. Fig. 10a shows that, in fact, the effect of superficial liquid velocity on the peak frequency is also approximately linear, but there is a non-zero intercept, corresponding to the critical velocity required for slug initiation.

The effect of pressure on slug frequency is demonstrated in Fig. 9. It can be seen that the pressure has no noticeable effect on the fully developed frequency, but that an increase in the pressure suppresses the initiation of slugs, so that the onset of slugging may be delayed, and the peak frequency reduced. These effects are more marked at lower superficial gas and liquid velocities. The effect of pressure on the peak and fully developed slug frequencies is summarized in Fig. 10b and c, which confirm that the pressure has no significant effect on the fully developed frequency. Fig. 10b shows that the reduction in the peak frequency with increasing pressure is more pronounced at a lower superficial liquid velocity for a given gas velocity. This is confirmed in Fig. 10c, where the reduction in peak frequency is only discernible at $U_{SG} \sim 2$ m/s.

The error bars on Figs. 7–9 show the irregularity in the arrival of slugs at each measurement position. This is quantified by recording the number of slugs arriving within a total of 30 intervals of 10 s each for a total experimental duration of 300 s. The error in estimating the mean slug frequency measured over 300 s is then estimated from the standard deviation of the 30 smaller sample means as

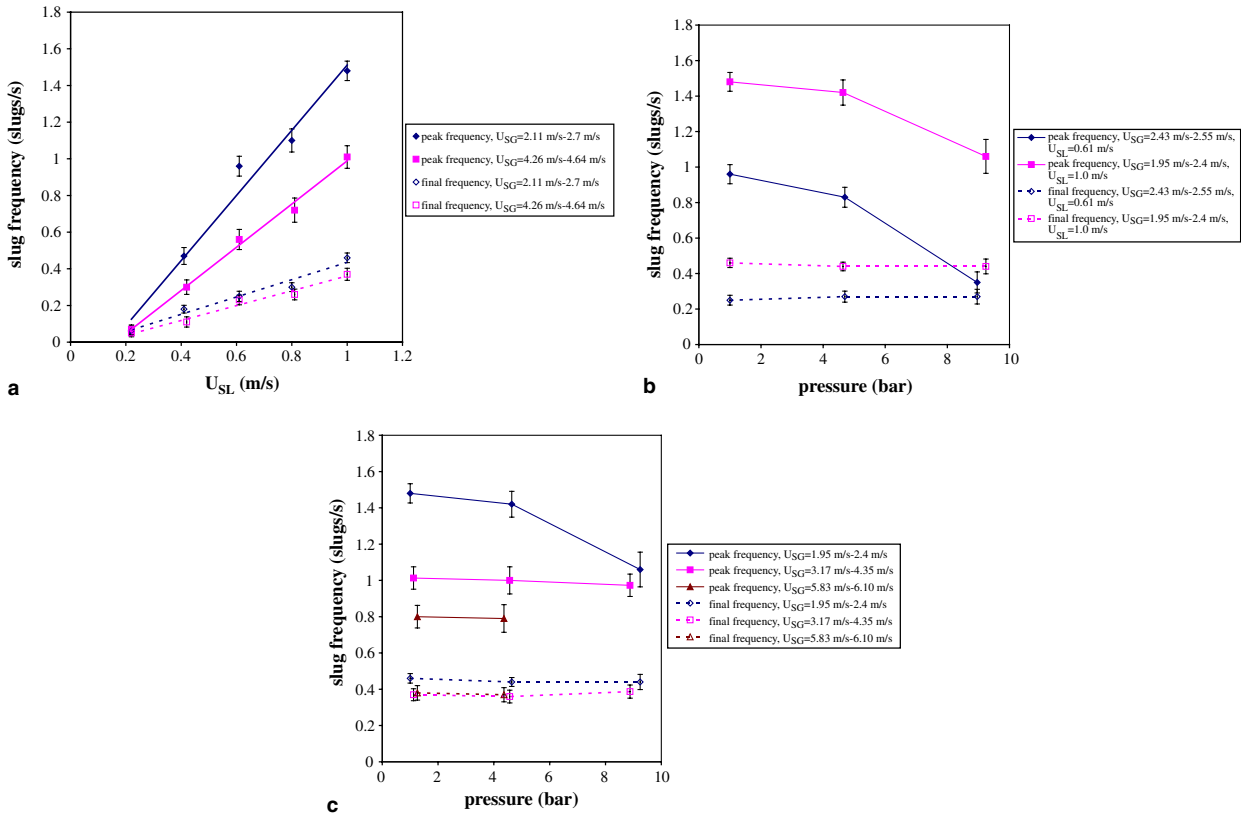

Fig. 10. (a) Variation of peak slug frequency (solid symbols) and fully developed slug frequency (open symbols) with superficial gas and liquid velocities; the effect of pressure on peak frequency (solid symbols) and fully developed frequency (open symbols) for: (b) $U_{SG} \sim 2$ m/s and $U_{SL} \sim 0.6$ m/s^{-1} m/s; (c) $U_{SL} \sim 1$ m/s and $U_{SG} \sim 3$–6 m/s.

$$\varepsilon[v_{300s}] \approx \frac{1}{\sqrt{30}}\varepsilon[v_{10s}] \tag{4}$$

The error bars show $\pm 2\varepsilon[v_{300s}]$.

6. Distribution functions for slug arrival times and lengths

Results are presented in this section to show the evolution of the distribution functions for slug body lengths and the time intervals between slugs, as well as the effects on these of the superficial liquid and gas velocities, and inlet pressure. The slug body lengths were obtained by multiplying the cross-correlation velocity of each slug and the interval between the arrivals of the subjectively identified slug front and tail.

Fig. 11 shows the evolution along the pipeline of the distribution of time intervals between slugs for three representative cases at near-atmospheric pressure. At the lowest superficial velocities (Fig. 11a, $U_{SL} = 0.41$ m/s, $U_{SG} = 2.36$ m/s), there is a peak at about 5 s, which gradually becomes dominant, with the short time intervals disappearing between 2 and 13 m downstream. Thereafter, there is little change in the distribution, apart from the appearance of a few longer intervals in the downstream region. When the superficial liquid velocity is increased to 0.61 m/s (Fig. 11b), the situation is similar, but the peak appears to shift from short times up to about 4 s; it does not stabilise until about 20 m, and the shorter intervals do not completely disappear. The appearance of longer intervals is also reduced, with little evidence of this until the final measurement position. When the superficial liquid velocity is maintained and the gas velocity is increased to 4.64 m/s (Fig. 11c), the distributions are similar to those at the lower gas velocity, but the peak is broader and consequently is lower in magnitude. Fig. 12 shows the effect of pressure on the evolution of the distribution of time intervals between slugs. The main effect is the suppression of slugs over the first few metres of the pipe at higher pressures. This leads to a broadening of the distribution, which is maintained all the way along the pipe.

Figs. 13 and 14 show the effects of superficial velocities and pressure on the evolution of the distribution of slug body lengths. As might be expected, the distribution of slug body lengths is similar to the distribution of time intervals between slugs; for given conditions of flow rates and pressure, longer time intervals tend to be followed by longer slugs. Fig. 13 shows that the overall distribution of slug lengths changes little with superficial gas or liquid velocity. A higher superficial liquid velocity tends to produce shorter slugs in the downstream region than a lower one (cf. Fig. 13a and b), with a complete disappearance of very short slugs there in the lower velocity case. An increase in superficial gas velocity also tends to produce shorter slugs in the downstream region (cf. Fig. 13c), but otherwise, it has very little effect on the shape of the distribution. Fig. 14 shows the distributions of slug body lengths for different values of the inlet pressure. The main feature is a significant peak in the distribution of slug lengths around $L_s/D = 10$, that persists further along the pipeline as the pressure is increased. This peak is present at the lowest pressure, but gradually subsides as short slugs decay and their liquid is swallowed up in the following slugs, which consequently become larger. At the highest pressure, the rate of decay is much lower, suggesting that the short slugs are more stable.

It is usually assumed that the lengths of slugs in fully developed flow follow a log-normal distribution (Barnea and Taitel, 1993; Bernicot and Drouffe, 1989, 1991; Dhulesia et al., 1991, 1993). Brill et al. (1981) used a log-normal distribution to describe the distribution of slug lengths at very large distances from the inlet in the Prudhoe Bay pipeline, and measurements reported by Nydal et al. (1992) indicated that slug lengths in shorter pipelines were also log-normally distributed. In addition, Dhulesia et al. (1991) fitted the inverse Gaussian or Wald distribution to data for slug body lengths. This is used to characterize the first passage time of an object and was first used for Brownian motion (Schrödinger, 1915). This interpretation can be extended to the analysis of slug flow data, where each slug can be treated as an ''object'' whose arrival at each measurement position is modeled. The authors assumed that the distance traveled by an individual slug could be represented by a Brownian motion with drift. It was further reasoned that the total liquid holdup in the pipeline is proportional to the accumulated length of slugs present. By considering the proportionality between the

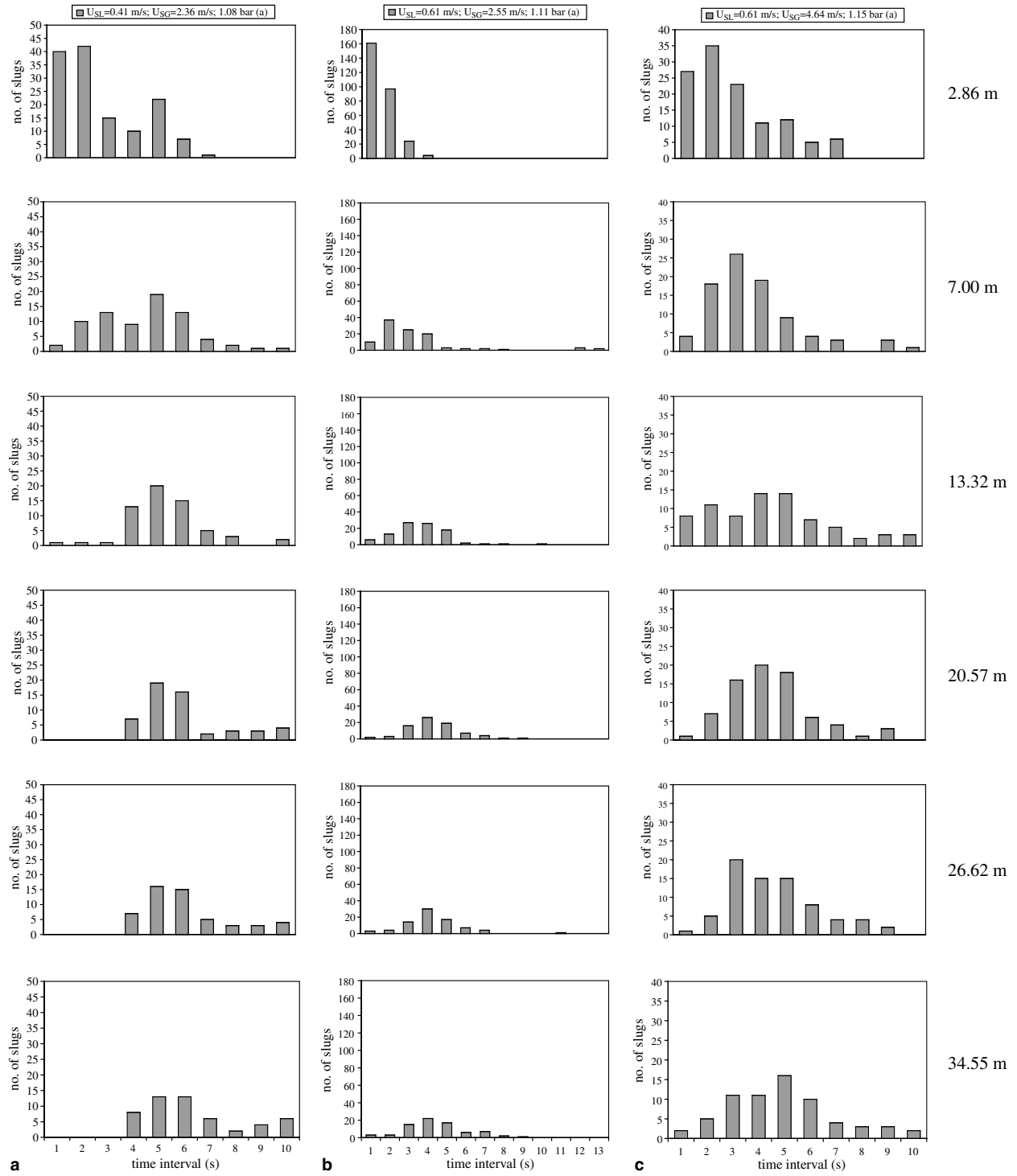

Fig. 11. Evolution along the pipeline of the distribution of time intervals between slugs: (a) $U_{SL} = 0.41$ m/s, $U_{SG} = 2.36$ m/s, inlet pressure = 1.08 bar(a); (b) $U_{SL} = 0.61$ m/s, $U_{SG} = 2.55$ m/s, inlet pressure = 1.11 bar(a); (c) $U_{SL} = 0.61$ m/s, $U_{SG} = 4.64$ m/s, inlet pressure = 1.15 bar(a).

accumulated slug length and the slug residence time, the authors concluded that the accumulated slug length may also be represented by an Inverse Gaussian distribution.

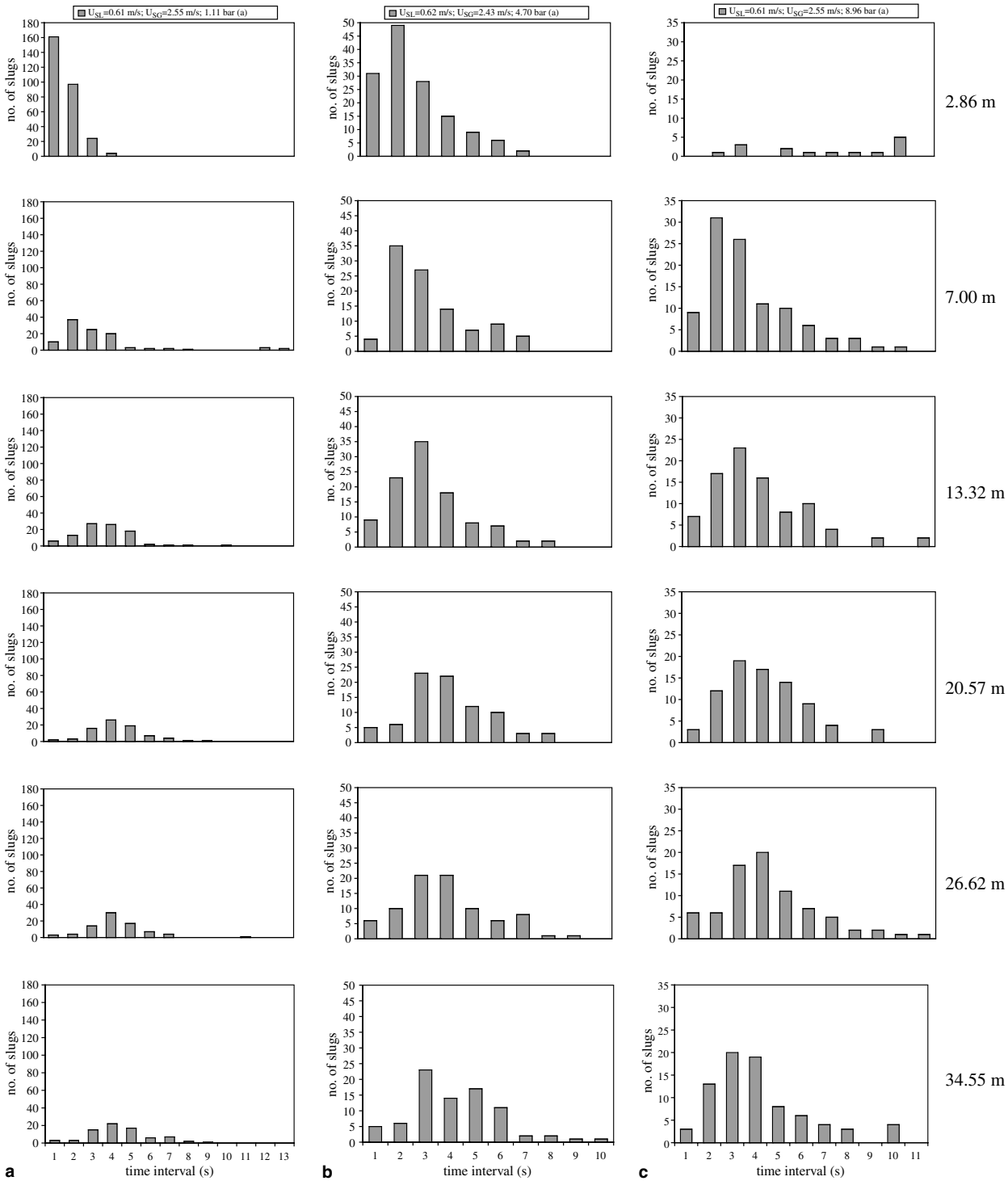

Fig. 12. The effect of inlet pressure on the evolution along the pipeline of the distribution of time intervals between slugs: $U_{SL} \sim 0.6$ m/s, $U_{SG} \sim 2.5$ m/s, (a) inlet pressure = 1.11 bar(a); (b) inlet pressure = 4.70 bar(a); (c) inlet pressure = 8.96 bar(a).

In the work of Ujang (2003), three continuous distributions, the normal or Gaussian, log-normal and inverse Gaussian, were fitted to the data for slug body lengths and arrival time intervals. A three-parameter

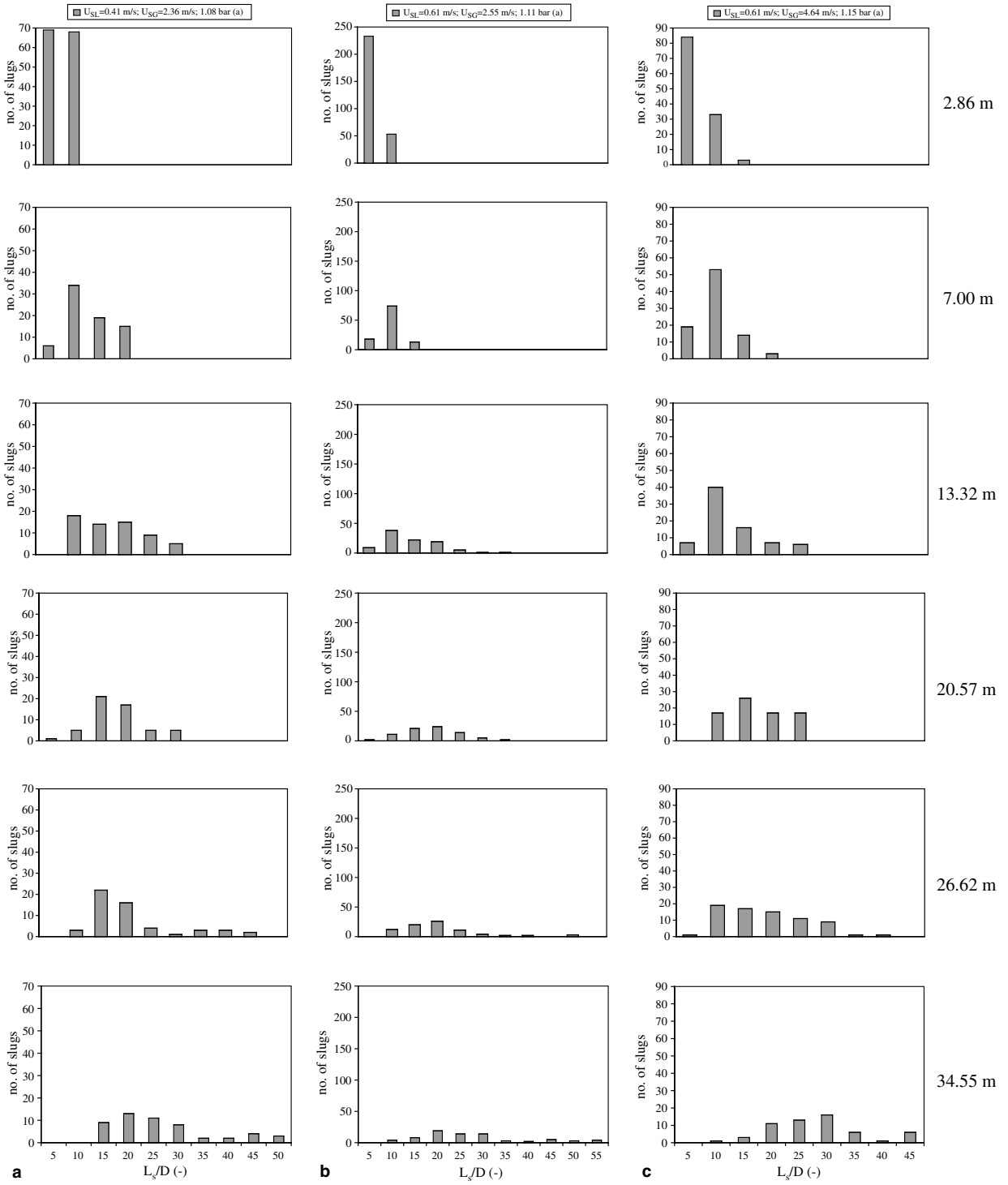

Fig. 13. Evolution along the pipeline of the distribution of slug body lengths: (a) $U_{SL} = 0.41$ m/s, $U_{SG} = 2.36$ m/s, inlet pressure = 1.08 bar(a); (b) $U_{SL} = 0.61$ m/s, $U_{SG} = 2.55$ m/s, inlet pressure = 1.11 bar(a); (c) $U_{SL} = 0.61$ m/s, $U_{SG} = 4.64$ m/s, inlet pressure = 1.15 bar(a).

version of the log-normal distribution was also considered. In addition, the exponential distribution was fitted to the data for arrival time intervals. This is the distribution that would apply if successive slug arrival times

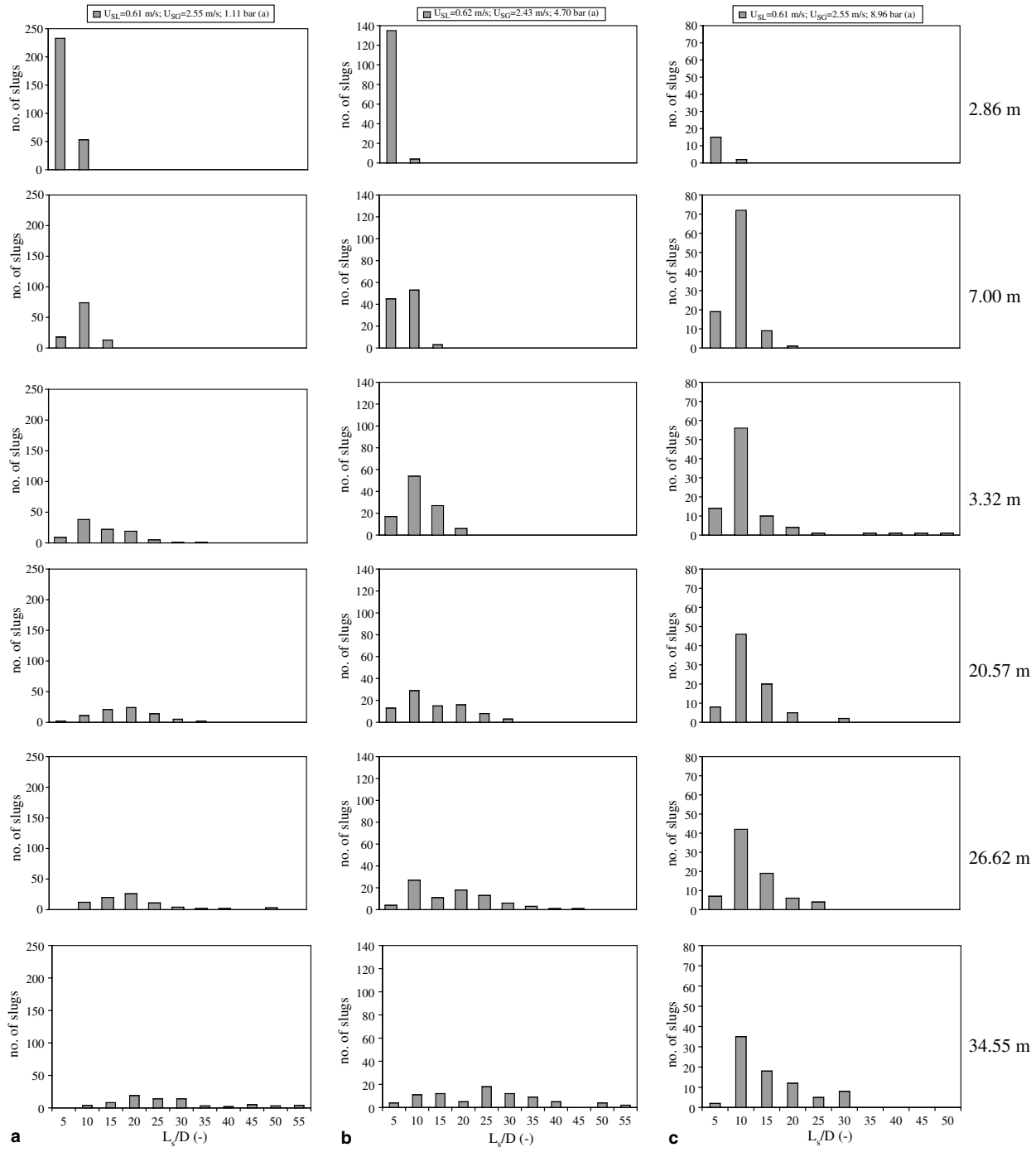

Fig. 14. The effect of inlet pressure on the evolution along the pipeline of the distribution of slug body lengths: $U_{SL} \sim 0.6$ m/s, $U_{SG} \sim 2.5$ m/s, (a) inlet pressure = 1.11 bar(a); (b) inlet pressure = 4.70 bar(a); (c) inlet pressure = 8.96 bar(a).

were uncorrelated, so that the number of slugs in a given time would be a Poisson random variable. Values for the parameters of each distribution were obtained using the method of maximum likelihood. Here we summarise the main findings of that analysis.

The expressions for the cumulative distribution functions of the distributions, and the best estimators for their parameters are as follows:

normal:

$$\Phi(x) = \frac{1}{\sqrt{2\pi}} \int_0^z \mathrm{e}^{-t^2/2} \mathrm{d}t = \frac{1}{2} \mathrm{erf}\left[\frac{x - \mu_G}{\sigma_G \sqrt{2}}\right] \tag{5}$$

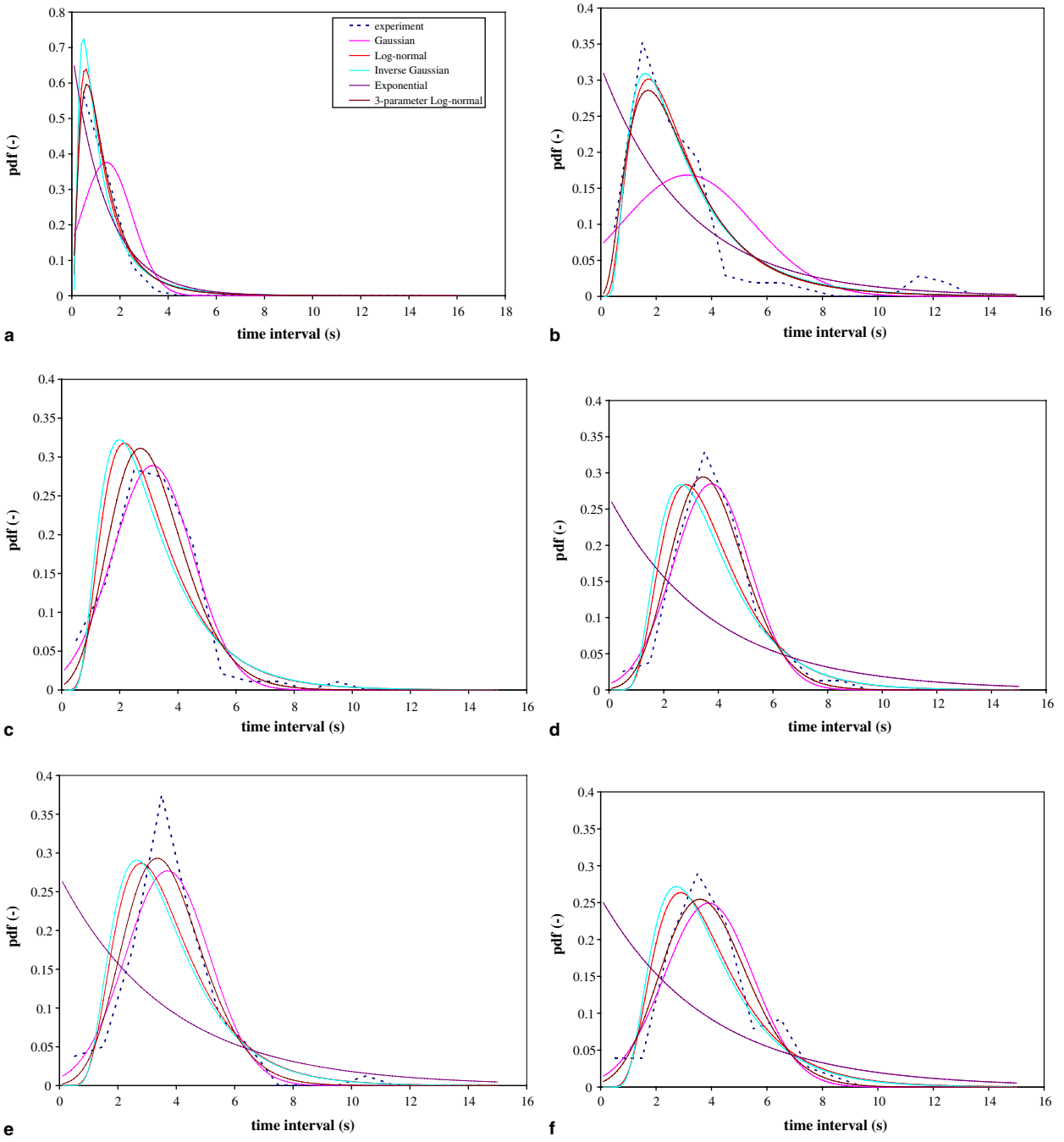

Fig. 15. Evolution of the sample distribution of the time interval between slugs and fitted distribution functions. $U_{SL} = 0.61$ m/s, $U_{SG} = 2.55$ m/s, inlet pressure = 1.1 bar(a).

with

$$\mu_G = \frac{1}{n}\sum_{i=1}^{n} x_i, \quad \sigma_G = \left[\frac{1}{n-1}\sum_{i=1}^{n}(x_i - \mu_G)^2\right]^{1/2}$$

log-normal:

$$\Phi(x) = \frac{1}{2}\mathrm{erf}\left[\frac{\ln x - \mu_{LN}}{\sigma_{LN}\sqrt{2}}\right] \tag{6}$$

with

$$\mu_{LN} = \frac{1}{n}\sum_{i=1}^{n} \ln x_i, \quad \sigma_{LN} = \left[\frac{1}{n}\sum_{i=1}^{n}(\ln x_i - \mu_{LN})^2\right]^{1/2}$$

inverse Gaussian:

$$\Phi(x) = \frac{1}{2}\mathrm{erf}\left[\frac{1}{\sqrt{2}}\left(\frac{\lambda_{IG}}{x}\right)^{\frac{1}{2}}\left(\frac{x}{\mu_G} - 1\right)\right] + \exp\left[\frac{2\lambda_{IG}}{\mu_G}\right]\frac{1}{2}\mathrm{erf}\left[\frac{1}{\sqrt{2}}\left(\frac{\lambda_{IG}}{x}\right)^{\frac{1}{2}}\left(\frac{x}{\mu_G} + 1\right)\right] \tag{7}$$

with

$$\lambda_{IG} = \left[\frac{1}{n}\left(\sum_{i=1}^{n}\frac{1}{x_i}\right) - \frac{1}{\mu_G}\right]^{-1}$$

Exponential

$$\Phi(x) = 1 - \exp\left(-\frac{x}{\mu_G}\right) \tag{8}$$

where erf is the error function.

For the one- and two-parameter distributions given in Eqs. (5)–(8), the fitting is simply a matter of evaluating the respective mean and standard deviation using experimental data for the slug lengths or for the time intervals between slugs. Three-parameter distributions allow for more accurate representation of data which are truncated on one side of the mean, in the present instance at zero. Fitting the parameters of these distributions is more involved and the reader is referred to the thesis of Ujang (2003) for full details.

The Kolmogorov–Smirnov test is used to investigate the significance of the difference between an observed continuous distribution and a specified population distribution (Massey, 1951). The test statistic is given by $\sup_x|F_n(x) - F_0(x)|$, which is the maximum difference between the cumulative distribution obtained from the sample, $F(x)$, and the cumulative distribution of the assumed population, $F_0(x)$. The test statistic is then compared with the standard Kolmogorov–Smirnov statistic, D_ϕ. If the test statistic is greater than D_ϕ, the null hypothesis that the sample came from the assumed population is rejected. Here ϕ is the level of significance of the rejection of the null hypothesis; a small value of ϕ means that the difference between the two distributions is highly significant. In the present work, we have taken ϕ to be 5%, and the corresponding values of D_ϕ, is $1.36/\sqrt{n}$, where $n > 35$ is the number of data in the sample. Samples of the goodness of fit assessment using the Kolmogorov–Smirnov test for each of the standard distributions, for the flow conditions given in Figs. 15 and 16 are given in Tables A1 and A2. The distributions which fail the test at the 5% confidence level are shown in bold in the tables.

Examples of the fitted distribution functions for the time interval between slugs are shown in Fig. 15, together with the experimental data for $U_{SL} = 0.61$ m/s, $U_{SG} = 2.55$ m/s and inlet pressure = 1.1 bar(a),

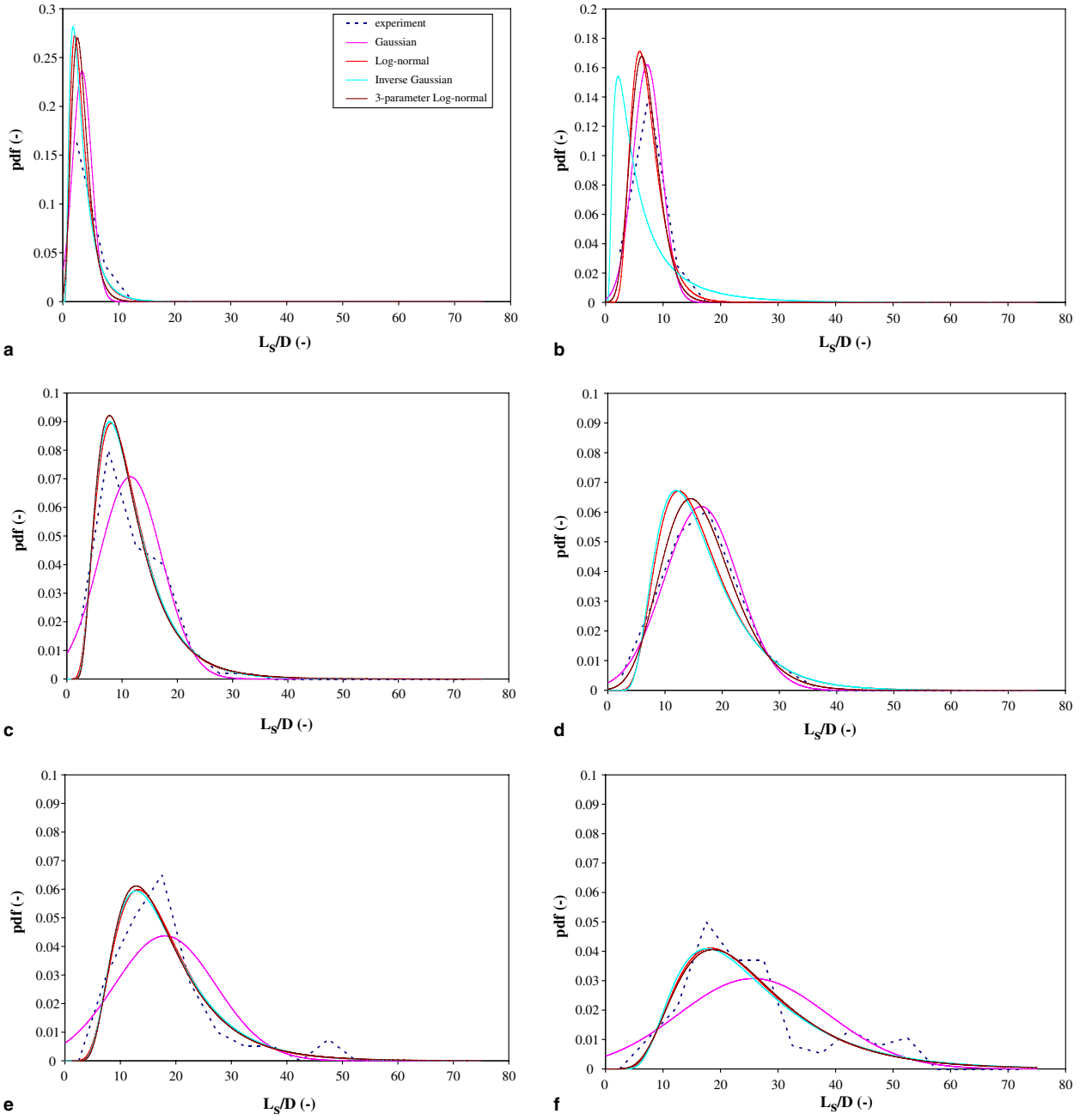

Fig. 16. Evolution of the sample distribution of dimensionless slug body lengths and fitted distribution functions. $U_{SL} = 0.61$ m/s, $U_{SG} = 2.55$ m/s, inlet pressure = 1.1 bar(a).

and the corresponding results obtained for the distribution of slug lengths are shown in Fig. 16. For clarity of presentation, the probability distribution functions are shown, which are simply the derivatives of the cumulative distribution functions given in Eqs. (5)–(8).

Each of the two-parameter distributions gave adequate fits to most of the data on the basis of the 1% and 5% Kolmogorov–Smirnov tests, but the best overall fits were obtained using the log-normal distribution. The three-parameter distribution, with an additional parameter, also allows the data to be accurately fitted.

However, we can conclude that the log-normal distribution, being simpler, is undoubtedly the best for practical purposes. The log-normal distribution sometimes fails to give an adequate fit to the distribution of time intervals in the inlet region, while the exponential distribution does gives an adequate fit in the region very near to the inlet, though the quality of the fit rapidly degrades with distance downstream. This indicates that slug initiation may be reasonably represented by an exponential distribution of arrival times, and hence a Poisson distribution of slug counts. This has the advantage that the distribution is determined entirely by a single parameter, the mean frequency, which is ideally suited to stochastic representations of slug initiation (Ujang, 2003).

In order to illustrate the variation of the distribution coefficients with position, values for the log-normal distribution coefficients are presented in Figs. 17 and 18, for the time interval and slug length data, showing the effect of gas and liquid flow rates, and pressure. In general, the mean time intervals and slug lengths increase steadily with distance, eventually reaching a fully developed state. The standard deviation of time-intervals tends to reduce with distance, reflecting the more regular slugs in the fully developed state. However, the standard deviation of slug lengths does not vary much with distance; the initial spread of lengths is preserved as the slugs propagate and grow. The mean of the time interval data does not appear to be significantly affected by the gas velocity, however an increase in liquid velocity leads to a significant reduction in the mean time interval. In the case of slug length, the mean is not strongly affected by either the gas or the liquid flow rate, though the slugs tend to be longer at lower superficial velocities. There is no discernible effect of flow rate on the standard deviation of slug lengths, while the standard deviation of arrival time intervals tends to increase with superficial velocity. The effect of pressure on the distribution parameters is shown in Fig. 18. The

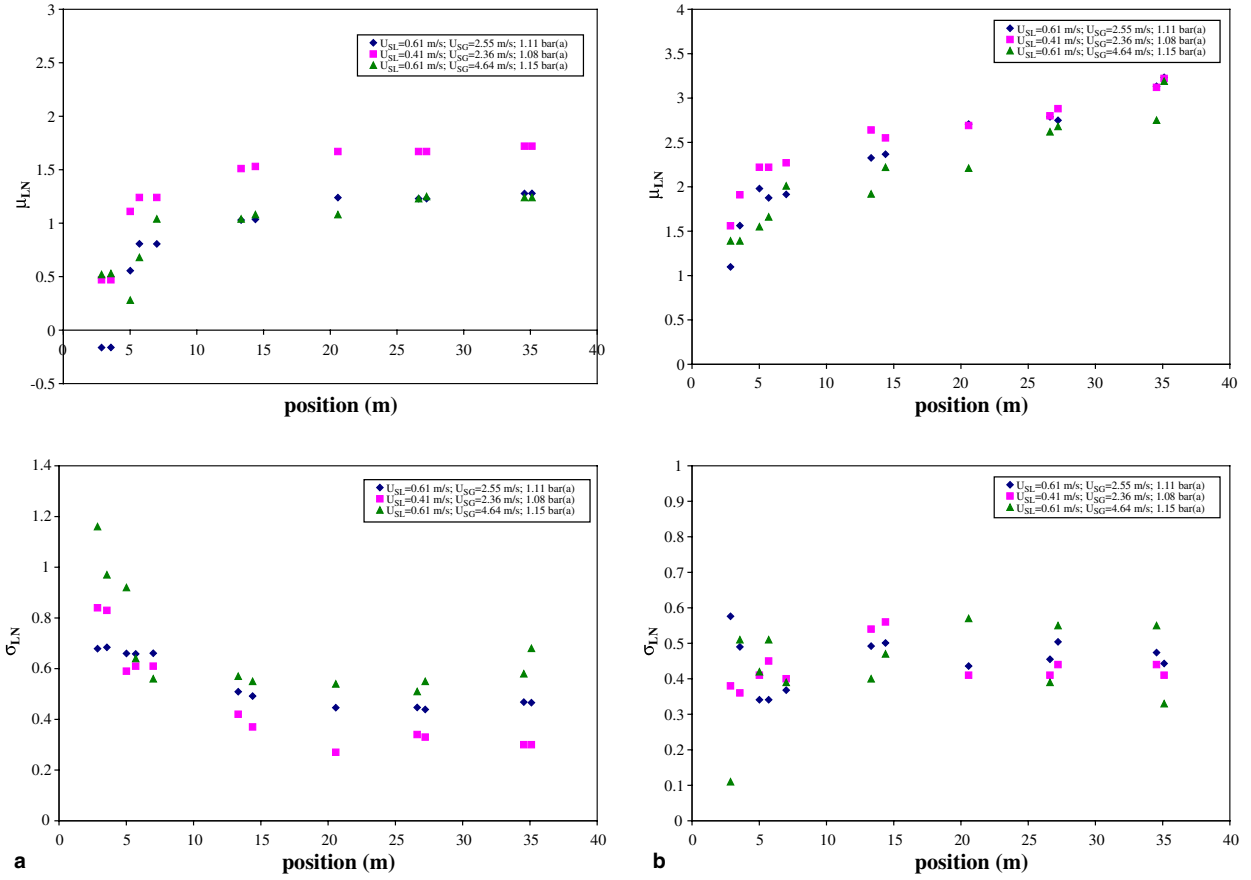

Fig. 17. Evolution of the log-normal distribution parameters with position showing the effect of superficial gas and liquid velocities: (a) time interval between slugs (s); (b) slug body lengths (m).

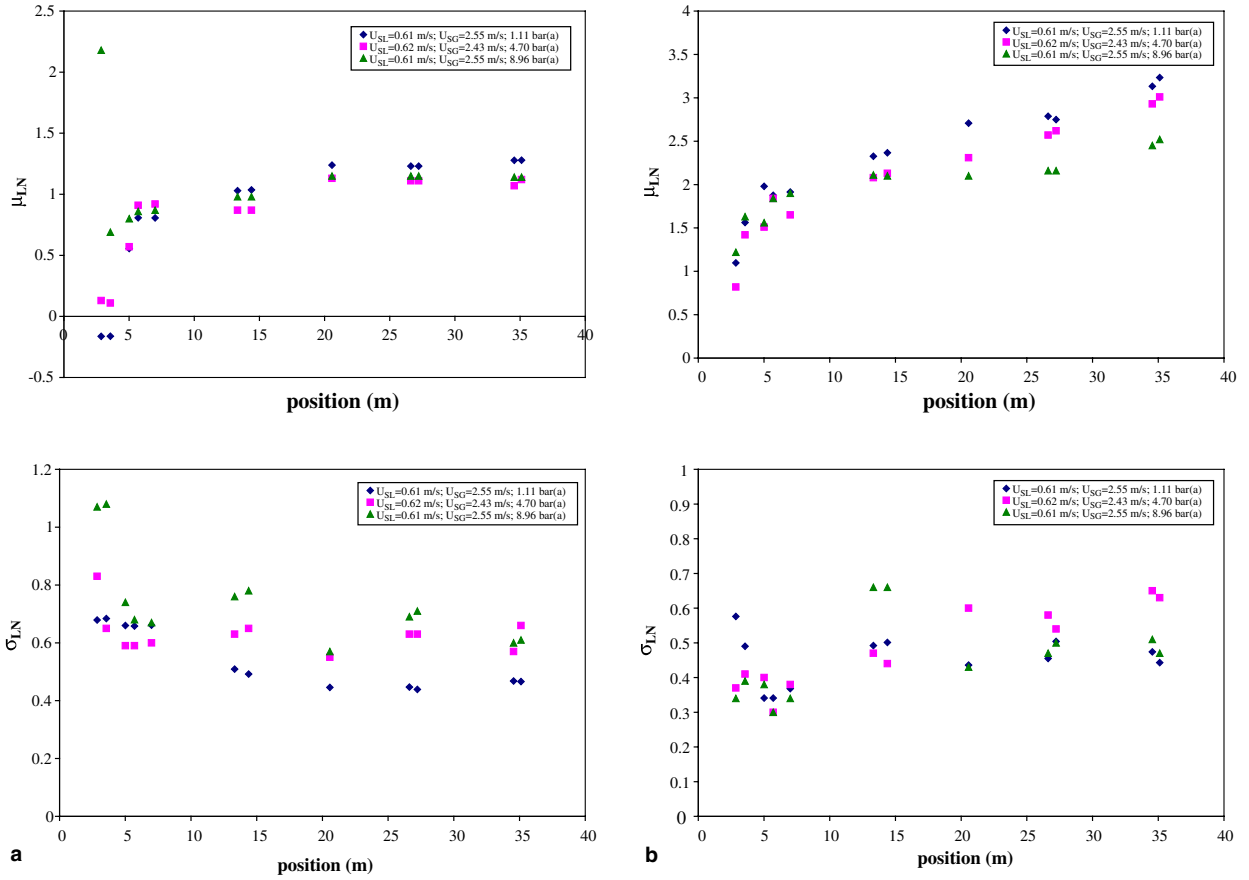

Fig. 18. Evolution of the log-normal distribution parameters with position showing the effect of pressure: (a) time interval between slugs (s); (b) slug body lengths (m).

suppression of slugs at the pipe inlet, discussed above is reflected in high values for the mean and standard deviation of the arrival time intervals at the first measurement point. The standard deviation remains somewhat higher along the pipeline, suggesting that the slug flow becomes slightly more irregular at higher pressure. The increase in pressure also seems to systematically reduce the mean slug length, while there is no discernible effect on the standard deviation of slug lengths.

7. Conclusion

New data have been presented for the distributions of time intervals between slugs and of slug lengths and, especially, the evolution of these distributions along a pipeline in slug flow. Both the liquid holdup associated with interfacial features and their translational velocity have been used in the identification and discrimination of slugs and waves. The data elucidate the separate effects of superficial liquid and gas velocities and system pressure on the processes of slug initiation and evolution.

Proposed mechanisms of slug initiation are confirmed by the data. It is clear that the liquid level immediately behind a newly initiated slug drops significantly below the level that existed ahead of the wave before it bridged the pipe. This level is then replenished by liquid flowing from the pipe inlet. Replenishment by a backward traveling wave from the tail of the slug precursor was not observed in these experiments. Many waves can be seen to grow on the rebuilding film but few of them will ultimately bridge the pipe. The survival of a slug precursor within the first 13 m of the flow was observed to be related to the thickness of the liquid layer

immediately ahead of it. If the level is too shallow, the front velocity of the precursor will be lower than the tail velocity, leading to its collapse back into a wave. It is this process that leads to a sometimes dramatic reduction in measured slug frequency within this region of the flow. The frequency of slug precursors increases with superficial liquid velocity, but decreases with superficial gas velocity. The fully developed slug frequency is just a fraction, typically 30–40% of this peak frequency.

Increasing the gas pressure has the effect of suppressing wave growth, so that slug initiation occurs further downstream. At higher pressures, the peak in slug frequency is lower, and is shifted downstream. However, further downstream, there was no observable effect of pressure on slug frequency. It can be seen that the initiation of slugs involves a combination of factors: the rebuilding of the liquid layer, the suppression or enhancement of suction at the top of the wave, and the distance for each slug precursor to grow to a stable length. The influence of pressure in retarding the initiation of slugs is possibly due to the reduction in the compressibility of the gas, so that pressure fluctuations near the inlet have less effect.

The statistical analysis of slug time intervals and lengths has indicated that these data are best represented by the log-normal distribution. It has also been shown that the slug time intervals measured very near the inlet are well-represented by an exponential distribution so that slug initiations can be considered as uncorrelated events. This is a useful observation, since only a single parameter (the mean frequency) is then needed for a stochastic representation of slug initiation. The mean time intervals and slug lengths tend to increase along the pipe; the standard deviation of time intervals decreases, while that of slug lengths does not vary systematically. The standard deviation of time intervals tends to increase with superficial velocity or pressure, suggesting that the fully developed slug flow is more irregular under these conditions.

Acknowledgements

The authors gratefully acknowledge the contributions made to this work by the Engineering and Physical Sciences Research Council (EPSRC) and the following industrial organisations: ABB, AEA Technology, BG International, BP Exploration, Chevron, Conoco, Enterprise Oil, Granherne, Institutt for Energiteknikk, Institut Français du Pétrole, Marathon Oil, Mobil North Sea, Norsk Hydro, Scandpower and TotalFinaElf. Prof. Christopher J. Lawrence gratefully acknowledges the support of Schlumberger and the Royal Academy of Engineering. The authors also wish to thank Mr. Malcolm Dix and Mr. Robert V. King and his staff for the provision of their expertise in the maintenance and upgrading of the WASP facility.

Appendix

See Tables A1 and A2.

Table A1
Maximum absolute deviations between actual and fitted cumulative distribution functions for time intervals between slugs

Distance (m)	No. of data, n	$\sup_x\|F_n(x) - F_0(x)\|$; $F_n(x)$ = actual cdf, $F_0(x)$ = fitted cdf					
		Gaussian	Log-normal	Inverse Gaussian	Exponential	3-Parameter log-normal	K–S D_ϕ (5%) test
2.86	207	**0.12**	0.06	**0.17**	**0.16**	0.06	0.09
3.56	245	**0.13**	0.05	0.08	**0.23**	0.06	0.09
5.01	134	0.12	0.07	0.10	**0.20**	0.05	0.12
5.70	95	0.13	0.08	**0.18**	**0.22**	0.08	0.14
7.00	95	0.13	0.08	**0.16**	**0.23**	0.07	0.14
13.32	95	0.08	0.10	0.13	**0.31**	0.08	0.14
14.39	95	0.08	0.10	0.10	**0.32**	0.07	0.14
20.57	79	0.08	0.12	0.15	**0.34**	0.06	0.15
26.62	80	0.08	0.13	0.15	**0.34**	0.07	0.15
27.22	80	0.09	0.11	0.13	**0.35**	0.08	0.15
34.55	76	0.07	0.07	0.10	**0.33**	0.05	0.16
35.11	76	0.07	0.07	0.10	**0.33**	0.05	0.16

$U_{SL} = 0.61$ m/s, $U_{SG} = 2.55$ m/s, inlet pressure = 1.11 bar(a).

Table A2
Maximum absolute deviations between actual and fitted cumulative distribution functions for slug body lengths

Distance (m)	No. of data, n	$\sup_x\|F_n(x) - F_0(x)\|$				
		Gaussian	Log-normal	Inverse Gaussian	3-Parameter log-normal	K–S D_ϕ (5%) test
2.86	208	0.08	0.07	**0.11**	0.05	0.09
3.56	246	0.04	**0.10**	**0.12**	0.04	0.09
5.01	135	0.06	0.07	0.08	0.05	0.12
5.70	95	0.05	0.10	0.11	0.05	0.14
7.00	95	0.06	0.05	0.06	0.04	0.14
13.32	95	0.12	0.07	0.06	0.07	0.14
14.39	95	0.12	0.05	0.05	0.05	0.14
20.57	79	0.08	0.08	0.10	0.06	0.15
26.62	80	0.16	0.07	0.08	0.07	0.15
27.22	80	0.15	0.07	0.08	0.06	0.15
34.55	78	0.18	0.09	0.09	0.10	0.15
35.11	78	0.13	0.04	0.05	0.05	0.15

$U_{SL} = 0.61$ m/s, $U_{SG} = 2.55$ m/s, inlet pressure = 1.11 bar(a).

References

Andritsos, N., Hanratty, T.J., 1987. Interfacial instabilities for horizontal gas–liquid flows in pipelines. Int. J. Multiphase Flow 13, 83–603.

Barnea, D., Taitel, Y., 1993. A model for slug length distribution in gas–liquid slug flow. Int. J. Multiphase Flow 19, 829–838.

Barnea, D., Taitel, Y., 1994a. Interfacial and structural stability of separated flow. Int. J. Multiphase Flow 20, 387–414.

Barnea, D., Taitel, Y., 1994b. Non-linear interfacial instability of separated flow. Chem. Eng. Sci. 49, 2341–2349.

Belcher, S.E., Hunt, J.C.R., 1993. Turbulent flow over hills and waves. Annu. Rev. Fluid Mech. 30, 507–538.

Benjamin, T.B., 1959. Shearing flow over a wavy boundary. J. Fluid Mech. 6, 161–205.

Bernicot, M.F., Drouffe, J.M., 1989. Slug length distribution in diphasic transportation systems. In: Fairhurst, C.P. (Ed.), Proceedings of the 4th International Conference on Multiphase Flow, Nice, 19–21 June, ISBN 0947711635, pp. 485–493 (Chapter 28).

Bernicot, M.F., Drouffe, J.M., 1991. A slug length distribution law for multiphase transportation systems. SPE Production Eng. 6, 166–170.

Brill, J.P., Schmidt, Z., Coberly, W.A., Herring, J.D., Moore, D.W., 1981. Analysis of two-phase tests in large diameter flow lines in Prudhoe Bay Field. SPE J. 8305, 363–377.

Crowley, C.J., Wallis, G.B., Barry, J.J., 1992. Validation of a one-dimensional wave model for the stratified-to-slug flow regime transition, with consequences for wave growth and slug frequency. Int. J. Multiphase Flow 18, 249–271.

Davies, S.R., 1992. Studies of Two-phase Intermittent Flow in Pipelines. Ph.D. Thesis, University of London.

Dhulesia, H., Bernicot, M., Deheuvels, P., 1991. Statistical analysis and modelling of slug lengths. In: Proceedings of 5th International Conference on Multiphase Production, Cannes, BHRA, Cranfield, Beds, pp. 80–112.

Dhulesia H., Hustvedt, E., Todal, O., 1993. Measurement and analysis of slug characteristics in multiphase pipelines. In: Proceedings of 6th International Conference on Multiphase Production, Cannes, June 16–18.

Dukler, A.E., Hubbard, M.G., 1975. A model for gas–liquid slug flow in horizontal and near horizontal tubes. Ind. Eng. Chem. Fundam. 14, 337–347.

Funada, T., Joseph, D.D., 2001. Viscous potential flow analysis of Kelvin–Helmholtz instability in a channel. J. Fluid Mech. 445, 263–283.

Hale, C.P., 2000. Slug Formation, Growth and Collapse. Ph.D. Thesis, University of London.

Hale, C.P., Hewitt, G.F., King, M.J.S., Lawrence, C.J., Manfield, P.D., Mendes-Tatsis, M.A., Odozi, U.A., Ujang, P.M., Wong, W.L., 2001. Slugs, waves and the law of the jungle. In: Proceedings of the 10th International Conference on Multiphase Production: Multiphase 01, Cannes, 13–15 June.

Hall, A.R.W., 1992. Multiphase Flow of Oil, Water and Gas in Horizontal Pipes. Ph.D. Thesis, University of London.

Issa, R.I., Kempf, M.H.W., 2003. Simulation of slug flow in horizontal and nearly horizontal pipes with the two-fluid model. Int. J. Multiphase Flow 29, 69–95.

Jeffreys, H., 1924. On the formation of water waves by wind. Proc. Roy. Soc. Lond. Ser. A 107, 189–205.

Jeffreys, H., 1925. On the formation of water waves by wind. Proc. Roy. Soc. Lond. Ser. A 110, 241–247.

Kordyban, E.S., 1985. Some details of developing slugs in horizontal two-phase flow. AIChE J. 31, 802–806.

Lighthill, M.J., 1962. Physical interpretation of the mathematical theory of wave generation by wind. J. Fluid Mech. 14, 385–398.

Lin, P.Y., Hanratty, T.J., 1986. Prediction of the initiation of slugs with linear stability theory. Int. J. Multiphase Flow 12, 79–98.

Lin, P.Y., Hanratty, T.J., 1987. Effect of pipe diameter on flow patterns for air–water flow in horizontal pipes. Int. J. Multiphase Flow 13, 549–563.

Manolis, I.G., 1995. High Pressure Gas–Liquid Slug Flow. Ph.D. Thesis, University of London.

Massey Jr., F.J., 1951. The Kolmogorov–Smirnov test for goodness of fit. J. Am. Stat. Assoc. 4, 1990.

McCready, M.J., 1998. Introduction to hydrodynamic stability. Lecture Notes (version 3/16/98), University of Notre Dame.

Nydal, O.J., Banerjee, S., 1996. Dynamic slug tracking simulations for gas–liquid flow in pipelines. Chem. Eng. Comm. 141–142, 13–39.
Nydal, O.J., Pintus, S., Andreussi, P., 1992. Statistical characterization of slug flow in horizontal pipes. Int. J. Multiphase Flow 18, 439–453.
Shaha, J., 1999. Phase Interactions in Transient Stratified Flow. Ph.D. Thesis, University of London.
Schrödinger, E., 1915. Zur Theorie der Fall- und Steigversuche an Teilchen mit Brownscher Bewegung. Phys. Z. 16, 289–295.
Srichai, S., 1994. High Pressure Separated Two-phase Flow. Ph.D. Thesis, University of London.
Taitel, Y., Dukler, A.E., 1976. A model for predicting flow regime transitions in horizontal and near-horizontal gas–liquid flow. AIChE J. 22, 47–55.
Taitel, Y., Dukler, A.E., 1977. A model for slug frequency during gas–liquid flow in horizontal and near horizontal pipes. Int. J. Multiphase Flow 3, 585–596.
Ujang, P.M., 2003. Studies of Slug Initiation and Development in Two-phase Gas–Liquid Pipeline Flow. Ph.D. Thesis. University of London.
Woods, B.D., 1998. Slug Formation and Frequency of Slugging in Gas–Liquid Flows, Ph.D. Thesis. University of Illinois at Urbana-Champaign.
Woods, B.D., Hanratty, T.J., 1999. Influence of Froude number on the physical processes determining frequency of slugging in horizontal gas–liquid flows. Int. J. Multiphase Flow 25, 1195–1223.